

Volume V Number 2 December 1974



GEOTECHNICAL ENGINEERING

Journal of

SOUTHEAST ASIAN SOCIETY OF SOIL ENGINEERING

Sponsored by

ASIAN INSTITUTE OF TECHNOLOGY

CONTENTS

Papers :	Page
Embankment Deformations due to Water Loads	
J.R. BOOKER and H.G. POULOS	73
Local Strains in Cylindrical Specimens of Kaolin during Consolidation	
A.S. BALASUBRAMANIAM	89
Long Piles under Tensile Loads in Sand	
R.H.S. TAN and T.H. HANNA	109
Technical Notes:	
An Arrangement for Measuring Swell Pressures Exerted by Expansive Soils	
NICHOLAS K. KUMAPLEY and GEORGE E. AFARI	125
Modified Failure Criteria for Sands	
T.S. NAGARAJ and B.V. SOMASHEKAR	133
International Society News	139
Southeast Asian Society News	140
Conference News	141
News of Publications	145
Asian Information Center for Geotechnical Engineering	147
Notes on Contributions to This Journal	149
Southeast Asian Society of Soil Engineering	150

EMBANKMENT DEFORMATIONS DUE TO WATER LOADS

J.R. BOOKER* and H.G. POULOS⁺

SYNOPSIS

A number of solutions are presented for the deformations and stresses within an embankment subjected to water loading. For a homogeneous embankment, the influence of water level, embankment slope and Poisson's ratio is investigated. The influence of a central core is also examined, and is found to be relatively small for the cases considered. It is further shown that the solutions for a homogeneous embankment may be used to estimate the movements within an embankment in which the modulus varies.

INTRODUCTION

Prediction of deformations in earth dams and embankments has become an almost routine procedure with the development of the finite element method. Despite the wide availability of suitable computer programs, there still exist many situations in which a computer is not available, or only a rapid estimate of deformation is required, or a study of the effects of parameter variations is desired. In a previous paper (POULOS et al, 1972), a series of solutions for the deformations of an embankment due to gravity forces has been presented and a method described for utilising these results to predict the deformations during construction. In the present paper dimensionless solutions are presented for the stresses and deformations within an embankment due to water loading acting on the upstream face, and a parametric study is made of the variables affecting the deformations. Such a study appears to be especially desirable in this case as, unlike the gravity loading case for which PENMAN et al (1971) have shown that a one-dimensional consolidation analysis can give a reasonable prediction of vertical movements during construction, simple approximations to obtain some idea of the order of magnitude of deformations are very difficult to devise.

Consideration is confined to the effects of the water acting as a load on the upstream face and no attempt is made to consider the effects of water loading on rockfill dams or to include the effects of saturation of the embankment on first filling, which in some cases, may be more significant than the loading effect. An attempt to incorporate the saturation effect into a finite element

* Senior Lecturer in Civil Engineering, + Reader in Civil Engineering, University of Sydney, Australia.

Discussion on this paper is open until 1 May, 1975.

BOOKER AND POULOS

analysis has been made by NOBARI & DUNCAN (1972). In addition, the analysis is not directly applicable to embankments or dams in which steady state flow conditions exist or which are subjected to rapid drawdown (these cases will be treated in a subsequent paper). Nevertheless, the results contained herein should be of relevance to embankments constructed at or above the optimum moisture content and to embankments or face dams having an impermeable upstream membrane.

ANALYSIS

In this paper the deformations due to water loading of a symmetrical embankment with a core, are considered. It is assumed that the embankment is sufficiently long that conditions of plane strain prevail, and a typical section is shown in Fig. 1. It is also assumed that both the embankment and the core may be considered elastic and that they rest on a rough rigid base.

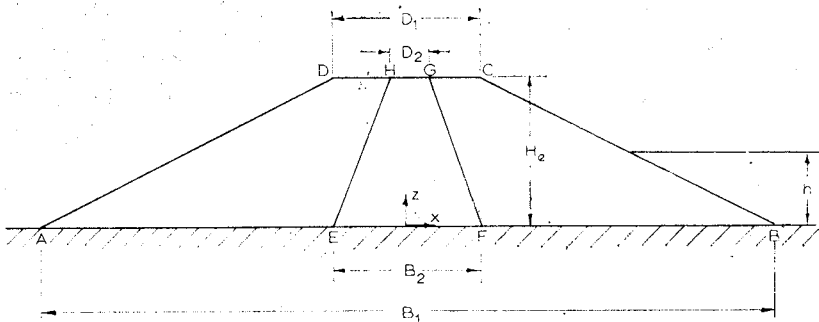


Fig. 1. Problem definition.

The following geometric and elastic parameters are used to describe the dam (see Fig. 1):

- B_1 = width of the base of embankment
- B_2 = width of the base of core
- D_1 = width of the top of embankment
- D_2 = width of the top of the core
- H_e = height of the embankment
- h = water height above base
- E = Young's modulus for the embankment shell
- E_c = Young's modulus for the core
- ν = Poisson's ratio of shell
- ν_c = Poisson's ratio for the core
- γ = unit weight of the material in the shell
- γ_c = unit weight of the material in the core
- γ_w = unit weight of water.

EMBANKMENT DEFORMATIONS

The behaviour of the embankment is therefore governed by a great many parameters, and in order to make this investigation tractable several of these parameters have been held constant at the following values:

$$\begin{aligned} B_2 / B_1 &= 0.2 \\ D_1 / B_1 &= 0.2 \\ D_2 / B_2 &= 0.25 \\ \gamma_c / \gamma &= 1 \\ \nu_c / \nu &= 1 \end{aligned}$$

The outer slope of the embankment θ , ν and the modular ratio E_c/E have been allowed to vary. The particular values chosen are "typical" and will serve to indicate practical trends in the behaviour of an embankment. For the purposes of obtaining a basic series of solutions, a "standard" homogeneous embankment was chosen, having the following parameters:

$$\begin{aligned} \theta &= 26.5^\circ (\tan^{-1}0.5) \\ H_e / B_1 &= 0.2 \\ \nu &= 0.4 \\ E_c / E &= 1 \end{aligned}$$

The stresses and displacements within the dam were found by means of a finite element analysis, using constant strain triangular elements. A typical finite element grid is shown in Fig. 2. The stresses and displacements due to water loading were calculated for several values of h/H_e . Since displacements are generally measured relative to the "in position" dam, only the displacements due to water loading are considered herein. The overall state of stress or displacement may be found by superposition of the solutions for water loading and gravity loading, provided that elastic conditions prevail.

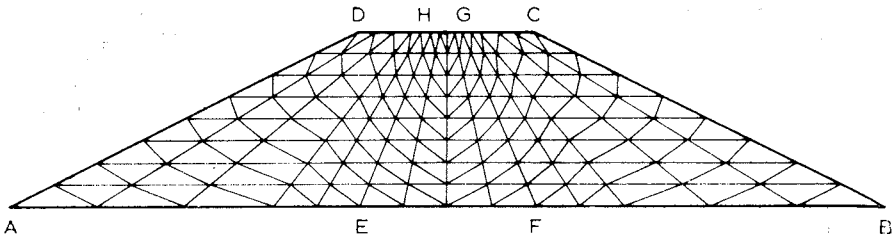


Fig. 2. Finite element representation.

SOLUTIONS FOR HOMOGENEOUS EMBANKMENTS

Stress and Displacement Contours for Standard Embankment

The first series of solutions was obtained for the homogeneous embankment described above, subjected to a "full pool" water loading. Dimensionless stress and displacement contours for this "standard" embankment are shown

BOOKER AND POULOS

in Figs. 3 to 7. An examination of these contours reveals that the largest stresses occur near the upstream toe of the embankment. The largest displacements occur at about the mid-height of the upstream face, the maximum vertical movement being approximately 60% of the maximum horizontal movement. In the down stream half of the embankment, relatively small stresses and displacements are developed. Figure 3 indicates that small tensile normal stresses are developed near the crest; however, it must be borne in

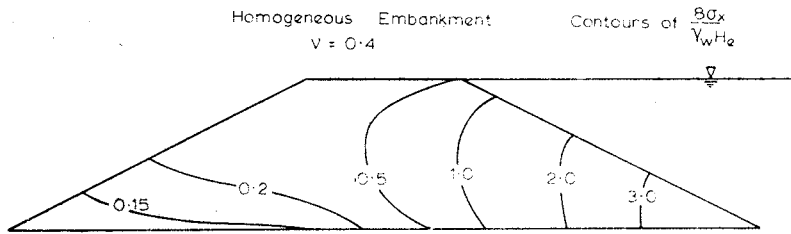


Fig. 3. Contours of horizontal stress σ_x (full pool).

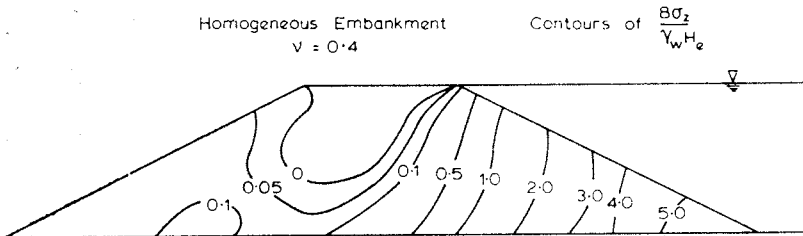


Fig. 4. Contours of vertical stress σ_z (full pool).

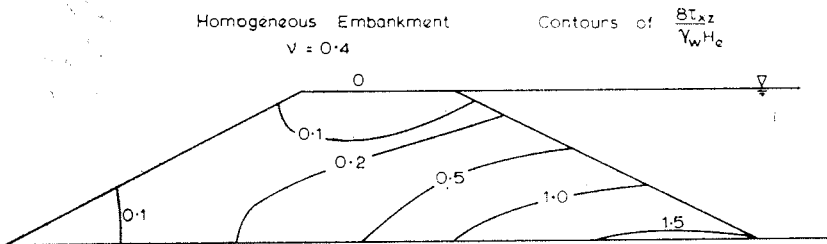


Fig. 5. Contours of shear stress τ_{xz} (full pool).

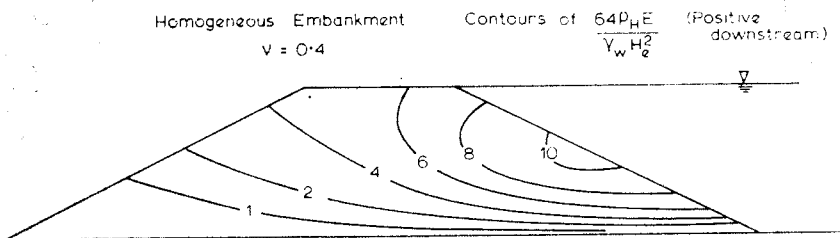


Fig. 6. Contours of horizontal movement ρ_H (full pool).

EMBANKMENT DEFORMATIONS

mind that these are only the stresses due to the water loading, and to obtain the overall stress field, the existing gravity stress field must be superimposed. The resulting stresses are compressive at all points within the embankment.

The effects of variations in a number of the parameters have been studied, including the water level, Poisson's ratio of the soil and the slope of the embankment. These effects are described below while the effects of a core within the embankment are considered subsequently. Because the movements at the crest are the most easily observed, attention will be largely concentrated on the vertical and horizontal deformations occurring at the centre of the crest.

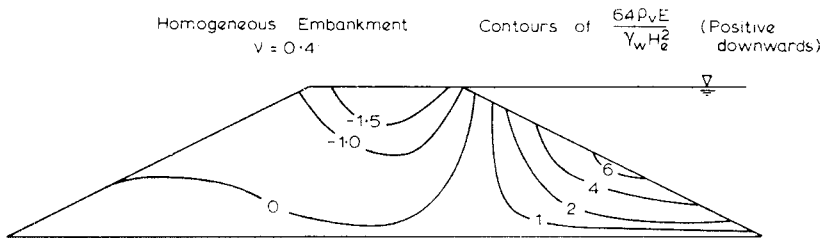


Fig. 7. Contours of vertical movement p_v (full pool).

Effect of Water Level

The variation with water level of horizontal and vertical displacements at the centre of the crest is shown in Figs. 8 and 9. The displacements are relatively small until the water level reaches about half the height of the embankment. Thereafter, an extremely rapid increase in movement occurs with increasing water level, especially the horizontal movement. For example, for the full pool condition ($h/H_e = 1$), the horizontal movement at the centre of the crest is about ten times the value at half pool ($h/H_e = 0.5$).

Figures 8 and 9 imply that relatively large fluctuations in movement may result from relatively small fluctuations in the water level behind the embankment under normal operating conditions. In real soils, such fluctuations in movement could result in progressive increases in irrecoverable movements with a consequent increase in the possibility of cracking.

Contours of vertical and horizontal displacement for the half pool conditions are shown in Figs. 10 and 11. Comparisons with Figs. 6 and 7 reveal that the movements at all points within the embankment are considerably smaller than for the full pool condition. The maximum movements again occur about half-way along the loaded part of the upstream face.

BOOKER AND POULOS

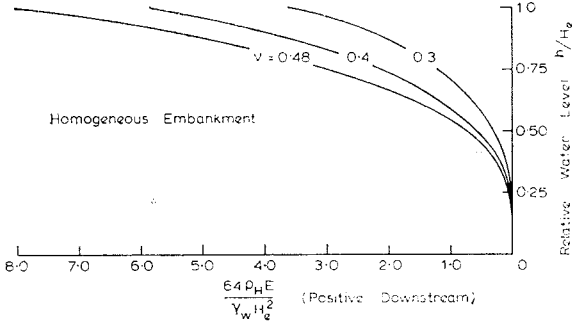


Fig. 8. Influence of water level and ν on horizontal movement at centre of crest.

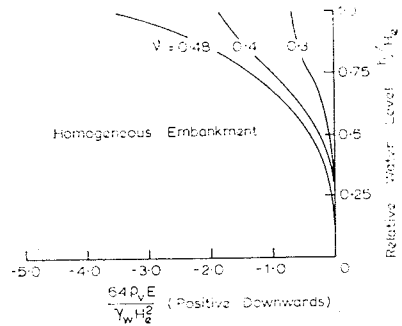


Fig. 9. Influence of water level and ν on vertical movement at centre of crest.

Effect of Poisson's Ratio of Material

Figures 8 and 9 also show the effect of Poisson's ratio of the embankment material on the crest movements. Both horizontal and vertical movements increase very significantly with increasing Poisson's ratio. This dependence of movements on Poisson's ratio precludes any simple consideration of the embankment as a cantilever in trying to obtain a rough estimate of horizontal deflection.

Effect of Slope

The effect of the side slopes on the crest movements is shown in Figs. 12 and 13 where the variation of movements with water level is given for three slopes. For all three slopes, the ratio B_2/B_1 has been held constant at 0.2. As would be expected, the movements increase very significantly as the side slope becomes steeper.

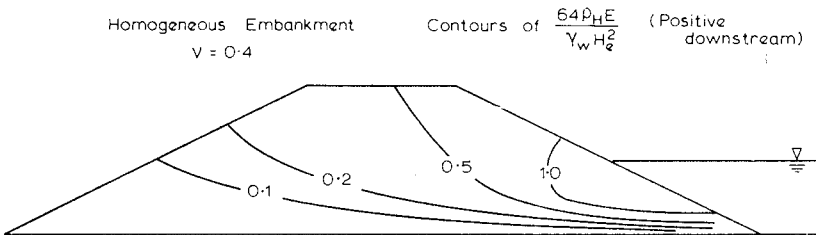


Fig. 10. Contours of horizontal movement ρ_H (half pool).

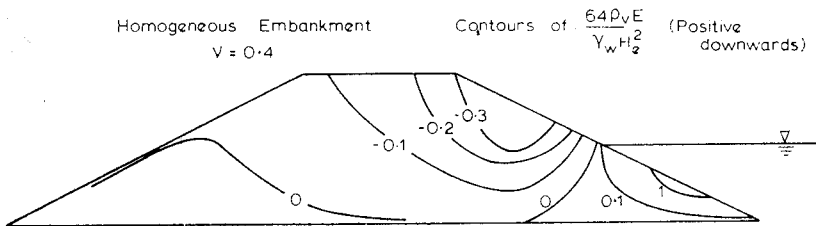


Fig. 11. Contours of vertical movement ρ_v (half pool).

EMBANKMENT DEFORMATIONS

Relative Magnitudes of Movements due to Water Loading and to Construction

In order to put the present solutions in perspective, a comparison between the vertical and horizontal movements due to full water loading and to construction has been made for a number of typical points within the "standard" embankment. The construction movements have been obtained from the solutions of POULOS et al (1972). The comparisons are shown in dimensionless form in Fig. 14. For the same value of E , the movements are of comparable order although the maximum vertical movement due to construction is about 50% greater than the maximum horizontal movement due to water loading. Actual measurements on three dams suggest that at points comparable to point D in Fig. 14, the horizontal movement due to water loading is considerably less than the horizontal movement due to construction. At Oroville Dam (NOBARI, & DUNCAN, 1972), the ratio of these movements is between 0.5 and 0.4 which agrees well with the theoretical value in Fig. 14 of 0.42. At Scammonden and Llyn Brianne dams (PENMAN & CHARLES, 1972) much smaller horizontal movements due to water loading were observed, although the presence of the core in the latter case may have largely influenced the construction movements. In addition, with real soils, the value of E relevant to construction is likely to be less than that relevant to water loading, thus reducing the relative magnitude of the movements due to water loading.

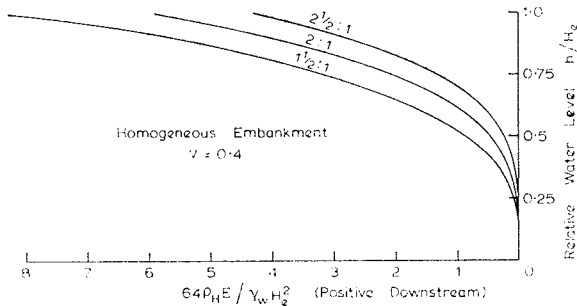


Fig. 12. Influence of side slopes on horizontal movement ρ_H at centre of crest.

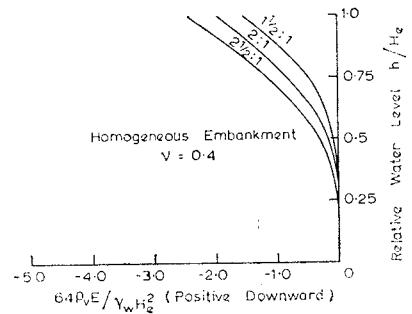


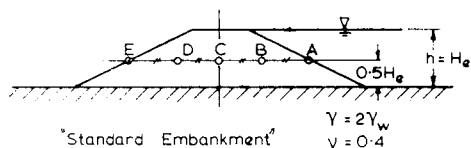
Fig. 13. Influence of side slopes on vertical movement at centre of crest.

SOLUTIONS FOR CORED EMBANKMENTS

In order to examine the influence of a core on embankment movements, the embankment shown in Fig. 2 was analysed, the overall dimensions of the embankment being the same as those of the standard embankment. The dimensions of the core were kept constant and the effect on movements of variations of the ratio of core modulus E_c to shell modulus E was examined. The water load was again taken to act on the upstream face.

BOOKER AND POULOS

For two typical cases, ($E_c/E=0.5$ and 2), contours of vertical and horizontal movements are shown in Figs. 15 to 18 for the full pool condition. Comparisons with Figs. 6 and 7 reveal that for the case $E_c/E = 0.5$, the vertical movements in the vicinity of the core are increased by about 40% but the horizontal movements are affected to a lesser extent. For the case $E_c/E = 2$, the vertical movements are again influenced more than the horizontal movements. In both cases, the effect of the core is relatively localised.



Point	Dimensionless Displacement I_p			
	During Const'n		Water Loading	
	Vert'l	Horiz'l	Vert'l	Horiz'l
A	·058	··066	·051	·087
B	·091	··057	·009	·067
C	·132	0	··007	·037
D	·091	·057	·002	·024
E	·058	·066	·000	·011

$$\text{Displacement } p = \frac{\gamma H_0^2}{E} \cdot I_p$$

Vertical displacements are positive downward
Horizontal displacements are positive downstream

Fig. 14. Theoretical relative magnitudes of movements due to construction and water loading.

The variation of the movements at the centre of the crest with water level is shown in Figs. 19 and 20 for five values of E_c/E . Although movements are reduced as the core becomes stiffer, the effect of increasing the core stiffness is remarkably small, especially in relation to horizontal movements. Similar small dependence on relative core stiffness is found for the vectorial movements of points on the upstream face, plotted in Fig. 21 for the full pool condition.

Although the effect of the core will increase as the size of the core increases, the solutions presented herein imply that for practical ranges of core size, the embankment movements due to water loading do not depend greatly on the relative core modulus.

NON-UNIFORM EMBANKMENTS

POULOS et al (1972) have suggested an approximate means of utilizing the solutions for a uniform embankment to predict construction movements of a non-uniform embankment and a similar approach can be adopted for the case of water loading. The assumption made is that the stress distribution within the non-uniform embankment is the same as that within the corresponding uniform embankment. Considering an embankment composed of various layers as shown in Fig. 22, the movement ρ_p at a point P may be approximated as follows:

EMBANKMENT DEFORMATIONS

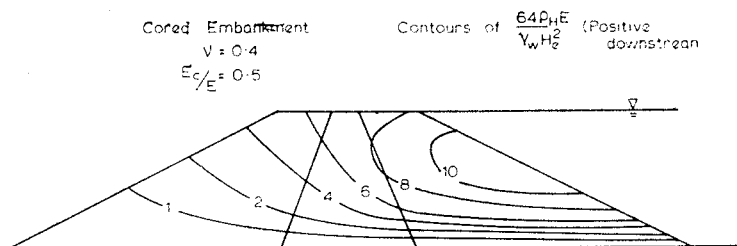


Fig. 15. Contours of horizontal movement ρ_H (cored embankment, full pool).

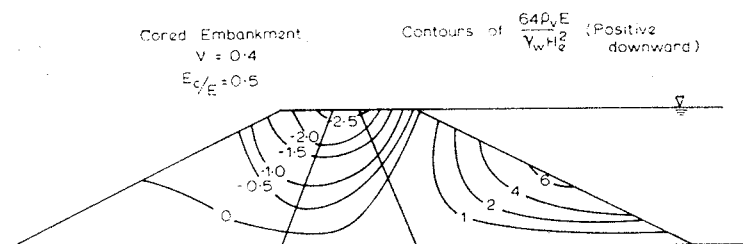


Fig. 16. Contours of vertical movement ρ_v (cored embankment, full pool).

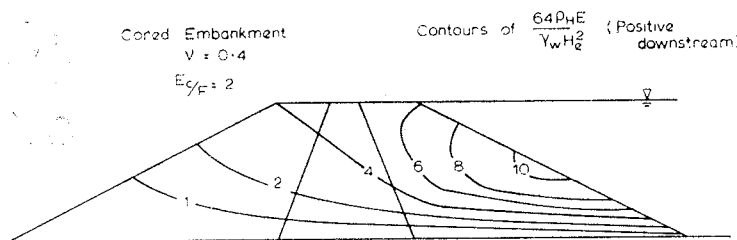


Fig. 17. Contours of horizontal movement ρ_H (cored embankment, full pool).

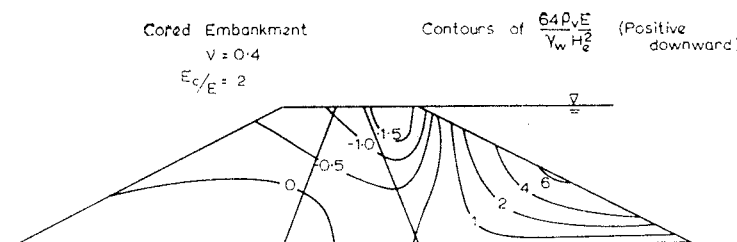


Fig. 18. Contours of vertical movement ρ_v (cored embankment, full pool).

$$\rho_p = \sum_{j=1}^n \frac{(I_j - I_{j-1})}{E_j} \gamma_w H_e^2 \dots \dots \dots (1)$$

where I_j = dimensionless movement influence factor for a point directly beneath P , at the top of layer j , distance z_j above the base.

E_j = Young's modulus of layer j

The influence factors I_j may conveniently be obtained from contour plots such as those shown in Figs. 6 and 7, and 15 to 18.

BOOKER AND POULOS

For a particular case, Fig. 23 shows a comparison between the approximate distribution of horizontal movement along the axis (using Eq. 1 and the homogeneous solutions in Fig. 6), and the correct solutions obtained from a finite element analysis using the specified variation of modulus with depth. Fig. 23 reveals quite good agreement between the two solutions, with the approximate solution giving a slight over-estimate of the movements. Thus, provided that large and abrupt variations in modulus with depth do not occur, the use of Eq. 1 with solutions for a homogeneous embankment should give reasonably reliable estimates of the movement of a non-homogeneous embankment.

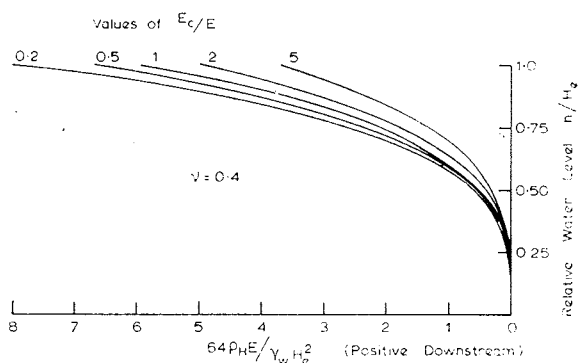


Fig. 19. Influence of core stiffness on horizontal movement at centre of crest.

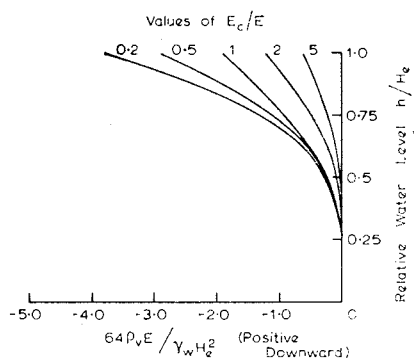


Fig. 20. Influence of core stiffness on vertical movement of centre of crest.

IMMEDIATE AND TOTAL FINAL MOVEMENTS

The theoretical results presented herein are most relevant to the following cases:

- (i) immediate or undrained movements of a relatively “wet” clay embankment due to water loading,
- (ii) immediate movements of an embankment subjected to rapid changes in water level, and
- (iii) immediate and long-term movements due to water loadings of an embankment with an upstream impermeable membrane.

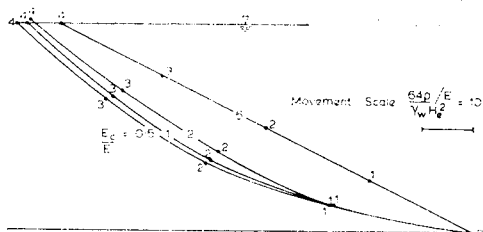


Fig. 21. Upstream movement profiles for cored embankment (full pool).

In calculating immediate or undrained movements, the relevant deformation parameters to use with the theoretical results are the undrained Young’s modulus E_u and undrained Poisson’s ratio ν_u . For long-term movements, the drained Young’s modulus \bar{E} and drained Poisson’s ratio $\bar{\nu}$ are used. Because of the

EMBANKMENT DEFORMATIONS

non-elastic behaviour of real soils these deformation parameters should be determined over a range of stress appropriate to the embankment being considered. This principle has been described in detail by LAMBE (1964) and DAVIS & POULOS (1963, 1968).

An interesting fact emerges from the theoretical solutions if the soil is assumed to be an ideal two-phase elastic material. In this case, the undrained Young's modulus E_u is related to the other parameters as follows:

$$E_u = \left(\frac{1 + v_u}{1 + \bar{v}} \right) \cdot \bar{E} \dots\dots\dots (2)$$

If this value of E_u and the appropriate theoretical solution for $v = v_u$ are used to determine the immediate horizontal crest movement due to water loading, and the value of \bar{E} and the theoretical solution for $v = \bar{v}$ are used to determine the total final movement, it is found that the immediate movement (downstream) is greater than the total final downstream movement. Thus, an upstream movement due to consolidation follows the immediate downstream movement. For real soils equation (2) may not hold accurately, and E_u and \bar{E} then need to be determined separately. In such cases, the above conclusions may need to be modified.

As a numerical example, an embankment of ideal two phase soil, 40 m high, 200 m wide at the base and having 1:2 side slopes will be considered, assuming the following parameters:

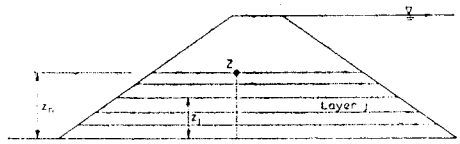


Fig. 22. Non-homogeneous embankment.

$$v_u = 0.48, \bar{v} = 0.3, \bar{E} = 10000\text{kN/m}^2, \gamma_w = 1 \text{ t/m}^3.$$

From equation (2), $E_u = 11380\text{kN/m}^2$, and using the dimensionless solutions in Fig. 8 with the appropriate E and v values, it is found that the immediate movement at the centre of the crest (downstream, for the full pool condition), is 176 mm, while the total final movement (downstream) is 92 mm, i.e. an upstream consolidation movement of 84 mm. will occur (assuming of course that no fluctuations in water level occur).

There appear to be very few cases in which long-term horizontal movements have been recorded, and in one case in which such movements are reported, E1 Infiernillo Dam (MARSAL & RAMIREZ, 1972), consolidation movements are downstream. However, it is very difficult to isolate the sources of such movements, and at least part of the downstream movement may be due to consolidation movements still occurring from the construction of the dam. Thus, at this stage, there appears to be no firm evidence to either confirm or contradict the theoretical conclusions reached above.

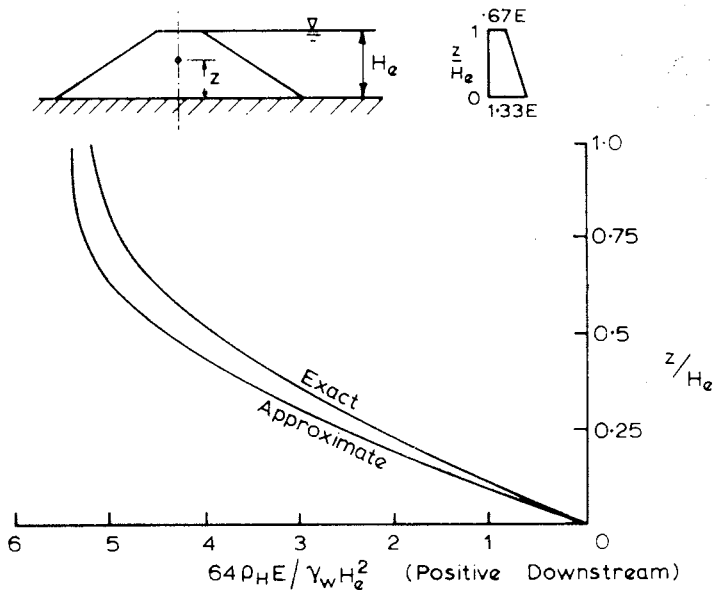


Fig. 23. Comparison between approximate and correct ρ_H on axis for non-homogeneous embankment.

OBSERVED AND THEORETICAL CHARACTERISTICS OF EMBANKMENT BEHAVIOUR

In this section, a brief review will be presented of some observations reported in the literature on embankment behaviour due to water loading and how this behaviour relates to the theoretical behaviour. The number of cases which are available is very small as there are only a few cases in which adequate measurements of embankment deformations have been made. Most of these have been on rockfill dams, for which as emphasized earlier, the solutions presented herein are only of limited validity because of the significant effects of saturation on first filling and also because the water loading cannot be considered to act on the upstream face. For these reasons and also because there is generally inadequate information on the relevant soil parameters, no attempt has been made here to obtain quantitative comparisons.

Possibly the most interesting series of observations with the present context are those on the Oroville Dam, summarized by NOBARI & DUNCAN (1972). Although this is a rockfill dam, it differs from many rockfill dams in that a high degree of compaction of the rockfill (100% relative density) was achieved, and also, an impervious section was situated upstream almost to mid-height. The possible effects of saturation and subsequent softening of the rockfill were therefore small. A plot of the measured horizontal movement at a typical point versus the water level is given in Fig. 24, and shows the same characteristics as the theoretical curves in Fig. 8, viz, a very rapid increase in

EMBANKMENT DEFORMATIONS

movement as the water level approaches the top of the dam. The tendency for movements to reverse direction at water levels between about R.L. 780 and 800 is probably associated with the fact that the rate of increase of the water level was not constant and that the water level increased very slowly between these two levels over a period of about 6 months. Consequently it is possible that some amount of upstream consolidation movements could have occurred during this time. Another feature of the measurements which showed agreement with the theoretical results was that the movements were smaller at points closer to the downstream face.

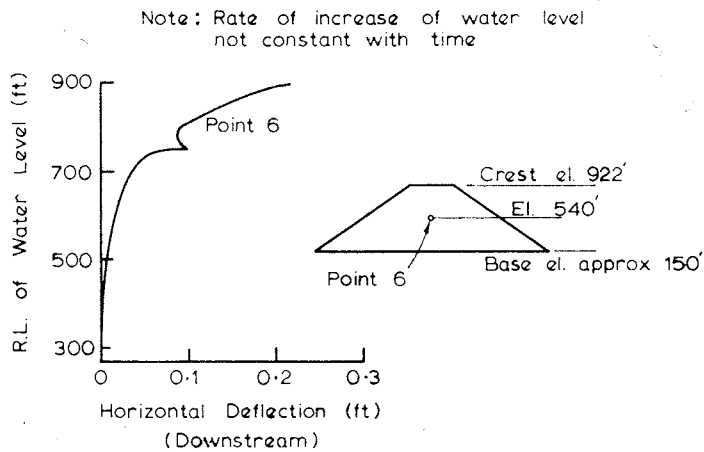


Fig. 24. Typical measured horizontal movements during filling at Oroville Dam. (After Nobari & Duncan, 1972)

Measurements of movements during first filling have also been made at a number of other dams e.g. El Infiernillo (MARSAL & RAMIREZ, 1967, 1972), Scammonden, and Llyn Brianne (PENMAN & CHARLES, 1972). In all these dams, upstream movements have been observed during the initial stages of filling followed by downstream movements as the water level approaches the top of the dam. As noted by (NOBARI & DUNCAN (1972), the early upstream movements could be a consequence of the effects of saturation of the rockfill. The effects of water loading begin to predominate in the later stages of filling, and the downstream movement increases rapidly as the water approaches its final level. Thus, apart from the saturation effects, the measured effects of water loading in the above three dams are consistent with the theoretical results.

FITZPATRICK et al (1973) have reported a number of observations on face dams with impermeable upstream membranes. Only upstream and downstream face deflection profiles for full pool conditions are reported, but the observed patterns of movement along the faces are similar to the theoretical

BOOKER AND POULOS

patterns. Along the upstream face, movements are relatively large with the maximum value occurring about half way up the face, whereas along the downstream face, the movements are considerably smaller. The observed and theoretical ratios of maximum normal upstream deflection to maximum downstream horizontal deflection agree quite well, but the observed downstream vertical movements are downwards whereas the theory predicts small upward movements. Nevertheless, the measured and theoretical characteristics of embankment deformation in the cases considered are sufficiently similar to suggest that the application of the elastic solutions presented herein may give a reasonable indication of the movements of embankments subjected to water loads, provided that the limitations stated in the paper are borne in mind.

CONCLUSIONS

A number of solutions have been presented for the deformations and stresses within an embankment subjected to water loading. A basic series of solutions has been obtained for a homogeneous embankment and the effects of water level, embankment slope and Poisson's ratio have been investigated. Deformations increase as embankment slope or Poisson's ratio increase, and very large increases in deformations occur as the water level approaches the top of the embankment. Some evidence of this phenomenon has been found in case records relating to earth dams.

A further inference of the results is that small fluctuations in water level at normal operating conditions could cause relatively large fluctuations in movement with a consequent increase in irrecoverable movements and an increase in the possibility of cracking. The influence of a central core has been studied and found to be relatively small for the range of relative modulus of core to shell likely to be encountered in practice. It has been further found that the solutions for a homogeneous embankment may be utilized to obtain an approximate estimate of the movements in an embankment in which the modulus varies with depth.

No attempt is made in this paper to consider the effects of water loading on rockfill dams or the movements arising from first filling due to saturation of the embankment material, which may be very significant in some cases. Similarly, cases in which conditions of steady flow are set up within the embankment are not treated. However, the results presented should have relevance to the estimation of undrained movements of clay embankments and of immediate and long-term movements of embankments with an upstream impermeable membrane.

EMBANKMENT DEFORMATIONS

ACKNOWLEDGEMENTS

The work described in this paper forms part of a general program of research into the settlement of all types of foundations being carried out at the University of Sydney under the general direction of Professor E.H. Davis, Professor of Civil Engineering (Soil Mechanics). The work is supported by a research grant from the Australian Research Grants Committee.

REFERENCES

- DAVIS, E.H. and POULOS, H.G. (1963), Triaxial Testing and Three-Dimensional Settlement Analysis, *Proc. 4th Aust.-New Zealand Conf. on Soil Mech. Found. Eng.*, pp. 233-243.
- DAVIS, E.H. and POULOS, H.G. (1968), The Use of Elastic Theory for Settlement Prediction under Three-Dimensional Conditions, *Geotechnique*, Vol. 18, pp. 67-71.
- FITZPATRICK, M.D., LIGGINS, T.B., LACK, L.J. and KNOOP, B.P., (1973), Instrumentation and Performance of Cethana Dam, *11th Int. Congr. on Large Dams.*, Q. 42, R. 9, pp. 145-164.
- LAMBE, T.W., (1964), Methods of Estimating Settlement, *J. Soil Mech. Found. Div., ASCE* Vol. 90, No. SM5, p. 43.
- MARSAL, R.J. and RAMIREZ DE ARELLANO, L. (1967), Performance of El Infiernillo Dam, 1963-1966, *J. Soil Mech. Found. Div. ASCE*, Vol. 93, No. SM4, pp. 265-289.
- MARSAL, R.J. and RAMIREZ DE ARELLANO, L. (1972), Eight Years of Observations at El Infiernillo Dam, *Proc. Conf. on Performance of Earth and Earth-Supported Structures*, ASCE, Vol. 1, pp. 703-722.
- NOBARI, E.S. and DUNCAN, J.M. (1972), Movements in Dams due to Reservoir Filling, *Proc. Conf. on Performance of Earth and Earth-Supported Structures*, ASCE, Vol. 1, pp. 797-815.
- PENMAN, A.D.M., BURLAND, J.B. and CHARLES, J.A. (1971), Observed and Predicted Deformations in a Large Embankment Dam during Construction, *Proc. Instn. Civ. Engrs*, London, Vol. 49, pp. 1-21.
- PENMAN, A.D. M. and CHARLES, J.A., (1972), Effect of the Position of the Core on the Behaviour of Two Rockfill Dams, *Bldg. Res. Stn. Current Paper CP 18/72*.
- POULOS, H.G., BOOKER, J.R. and RING, G.J. (1972), Simplified Calculation of Embankment Deformations, *Soils and Foundations*. Vol. 12, No. 4, pp. 1-17.

LOCAL STRAINS IN CYLINDRICAL SPECIMENS OF KAOLIN DURING CONSOLIDATION

A.S. BALASUBRAMANIAM*

SYNOPSIS

This paper summarises the method adopted and the local strains measured in cylindrical specimens of kaolin 1.5 inch and 4 inch diameter during one dimensional consolidation and subsequent isotropic consolidation. The local strains were measured by an X-ray technique where the strains were determined from the displacement of lead shot markers embedded in the clay. Since it is customary to prepare remoulded specimens of clay by one dimensional consolidation and subsequent isotropic consolidation prior to shear in the conventional triaxial apparatus, the results presented here will be of value in ascertaining the uniformity of the sample at the end of consolidation and prior to shear. From the local strains, local voids ratios are calculated and from these values pore pressure isochrones are determined. The results also indicated that for isotropic stresses of similar magnitude to the initial one dimensional stress, the strains induced by increments of isotropic stresses were anisotropic. However, for specimens which were isotropically consolidated to approximately three times the initial one dimensional stress the effect of anisotropy was found to be small.

INTRODUCTION

Non-destructive technique using X-rays has been developed for the determination of internal strains and voids ratio in cylindrical specimens of kaolin during one dimensional and isotropic consolidation. The method is used to study the local deformation as well as to check the uniformity of deformation.

An X-ray technique was first developed by ROSCOE et al (1963) for determining the strain patterns under plane strain conditions from the measurements of the displacements of lead shot markers embedded in sand. The method was subsequently modified and used by SIRWAN (1965) for the measurement of local strains in triaxial specimens of sand during shear. BURLAND (1967) and BURLAND & ROSCOE (1969) described the local strains during one dimensional consolidation of kaolin in a model clay footing. This paper summarises the method adopted and the local strains measured in cylindrical specimens of kaolin 1.5 inch and 4 inch diameter during one dimensional consolidation and subsequent isotropic consolidation. Since it is customary to subject remoulded specimens of clay to one dimensional and

* Assistant Professor of Geotechnical Engineering, Asian Institute of Technology Bangkok, Thailand.

Discussion on this paper is open until 1 May, 1975.

BALASUBRAMANIAM

isotropic consolidation prior to shear in the conventional triaxial apparatus, the results presented here will be of value in ascertaining the uniformity of the sample at the end of consolidation.

In addition to the measurement of local strains, the side friction between the clay and the surface of the former in which the clay is consolidating is assessed by making use of a load cell at the base of the sample.

APPARATUS

Consolidometer

The consolidometer was mainly used for X-ray work. Hence it was essential to select a material which has an absorption coefficient which is as small as possible. Perspex and aluminium were selected because of their relatively low X-ray absorption coefficients.

The description of the way in which the pedestal of the base of a commercially available triaxial cell was modified to incorporate a load cell has been given by BURLAND (1967). The special consolidometer used to study the uniformity of strains during one dimensional consolidation of the clay is shown in Fig. 1. It consists of a perspex tube made in two parts and connected by a collar. The internal face of the tube is highly polished and is 1.5 inch diameter. The two parts are held together by two metal end plates connected by four screwed rods L. The bottom metal plate forms a seal against the rubber cap on the pedestal containing the load cell. The piston M is made of PTFE to reduce friction between it and the side walls. Its lower face contains a porous stone (3/16 inch thick and type UNI 150 KV) and this is the only drainage face for the sample. The cassette N for the X-ray films rests in a special holder with reference markers such as P fixed in rows on both sides of this holder. The whole apparatus is mounted on the square base plate Q which can be fixed at one end of a test bed while the X-ray head is mounted at the other end. Loads are applied to the piston M by a hanger.

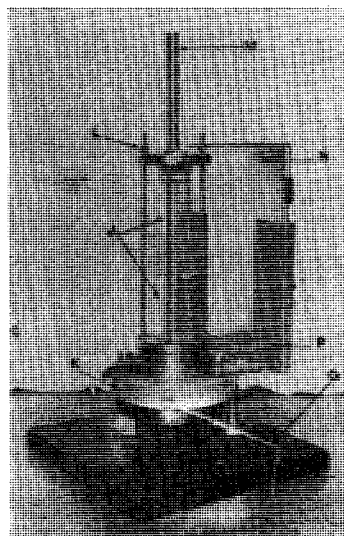


Fig. 1. Perspex consolidometer.

One test, to investigate the effects of side friction during one dimensional consolidation was carried out with the perspex tubes replaced by tubes of duralumin.

LOCAL STRAINS DURING CONSOLIDATION

When not wishing to study deformation during one dimensional consolidation, clay samples were prepared in an adaption of the sand sample formers made by THURAIRAJAH (1961). This former is described in BALASUBRAMANIAM (1969).

Experimental Set Up for Taking Radiographs

All tests with radiographic work was carried out in an X-ray compound shielded with double-lined lead screens. With 1.5 inch diameter samples a focal film distance of 4 feet was found to be necessary for good definition of the images of the lead markers on the radiographs. Test beds six feet long were made. The 1.5 inch triaxial cells were each mounted on a special base plate with a highly polished upper surface covered with a thin layer of lubricant. The 1.5 inch triaxial cell could then be rotated about a vertical axis and could be clamped in two mutually perpendicular directions. The cassette holder was mounted on the same base plate at the back of the triaxial cell. Two vertical columns of lead markers, each 0.080 inch diameter were fixed to both sides of the cassette holder. The images of these markers were used as references to locate the true axes of the triaxial system in the radiographs. The triaxial cell pressure was supplied through a flexible pressure tubing connecting to the base of the triaxial cell. The X-ray head was mounted on a plate similar to the triaxial cell but on the other end of the same test bed. The position of the two base plates could be varied along the length of the test bed.

Sample Preparation

Air-dried kaolin was mixed with 160% of distilled water in a commercial pugmill for about three hours under a vacuum of 20 inches of mercury. The properties of kaolin are liquid limit = 74%, plastic limit = 42%, plasticity index = 32% and specific gravity = 2.61. The kaolin slurry was carefully placed in the consolidation former with a long handled spoon. A perspex jig and a probe are used for placing the lead markers in the clay. The perspex jig can be slid into the top of the consolidometer former so that it is located by the two pins projecting above this former. The lower surface of the jig is then nearly in contact with the upper surface of kaolin. The holes in the jig are spaced in a manner in which any desired pattern of lead markers can be arranged in two mutually perpendicular directions. The probe has a small cavity at one end in which the lead markers sit while being forced down to their respective positions. This method of placing lead markers was found to be satisfactory even with the four inch diameter sample in which some of the lead markers were located correctly at a depth of 17 inches below the jig.

Equipment for Non-destructive Tests

The X-ray equipment used was a Meuller M.G. 150 Industrial set. Detailed description of the set is given by JAMES (1965). Briefly the X-ray set can be operated with a fine focal spot of 1.5 mm or a coarse focal spot of 4 mm. The maximum range of tube voltage was from 50 kV to 150 kV. The maximum tube current was 20 milliamp with the coarse focal spot and 8 milliamp with the fine focal spot. The input voltage was stabilised within 0.1 % using a regulator in the range 190 to 260 volts.

Kodak Industrex type D films were used for most of the radiographs. The film was placed between two lead screens (0.004 inch thick at the back and 0.006 inch thick in the front) inside a standard Kodak steel cassette.

The exposure time was selected by trial and error to obtain an optimum film density of 1.0 as suggested by JAMES (1965). The exposure time used for the one dimensional consolidation tests on 1.5 inch diameter samples varied from 1.5 to 2 minutes at 70 kV with a tube current of 15 mA and the fine focal spot. A focal film distance of 50 inches was employed. Approximately identical exposure conditions were used for all triaxial work on 1.5 inch diameter samples. Two types of exposure conditions were employed with the four inch diameter samples depending on the focal film distance (f.f.d.). With f.f.d.'s of 50 and 120 inches, exposures of 4 mA for one minute and 6 mA for 8 minutes at 130 kV were used.

The exposed films were developed in DX-80 developer for four minutes. The films were agitated while being developed for about 10 times at the end of each minute. The films were then fixed in acid fixative for 12 minutes. Afterwards they were washed in running water and dried. The developed films were kept in boxes and stored in a cool dark place.

Measurement of the Positions of the Images of the Lead Markers on the X-ray Films

The radiographs taken in the earliest tests carried out were measured in the orthogonal displacement meter described by ROSCOE, et al (1963). Subsequent measurements were carried out 1965 in the Cambridge University, Cavendish Laboratory using a machine (called CLARA) which is described in detail by LORD (1969). Late in the test programme a new measuring machine designed and developed by JAMES (1965) in the Cambridge University Engineering Laboratory became available and was used for all measurements on the 4 inch diameter samples.

LOCAL STRAINS DURING CONSOLIDATION

In the 1.5 inch diameter samples the lead markers were arranged in two mutually perpendicular vertical planes containing the axis of the sample as shown in Fig. 2. This method was adopted to be able to compare the strains from one plane with those in the orthogonal plane.

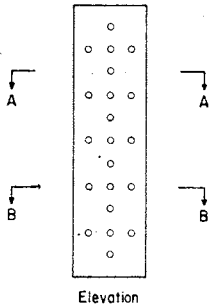
With the 4 inch diameter samples, again the lead markers were arranged in two perpendicular planes. The number of columns in any one plane varied from 6 to 9 while the number of rows varied from 8 to 16. The computation of the coordinates of each marker is described in detail in BALASUBRAMANIAM (1969).

Two methods were adopted for the calculation of strains from the displacement of the lead markers. In the first method the axial and radial strains were computed directly from the axial displacements and the radial displacements of four markers lying in the same vertical plane. The axial strain ϵ_y and the radial strain ϵ_x are given by :

$$\epsilon_x = \log \left[\frac{(x_1 - x_2)}{\left\{ (x_1 - x_2) + (c_1 - c_2) \right\}} \right]$$

$$\epsilon_y = \log \left[\frac{(y_3 - y_4)}{\left\{ (y_3 - y_4) + (d_3 - d_4) \right\}} \right]$$

where x_1, x_2 are the x coordinates of the markers in the same horizontal plane and c_1 and c_2 are the corresponding displacements in the x direction. y_3 and y_4 are the y coordinates of the markers in the same vertical line and d_3, d_4 are their corresponding displacements.



In the second method the strains were computed from the displacements of three markers, by assuming a linear homogeneous function for the displacement in terms of the coordinates.

The general assumptions made in the derivation of strains from the measurements of displacements of lead shot markers are (i) the mass of soil within the smallest grid deforms uniformly and (ii) there is no relative movement between the lead markers and the surrounding soil. The experimental observations in support of these assumptions have already been presented for sand by ROSCOE et al (1963). The validity of these assumptions for clay will be considered in the latter sections.

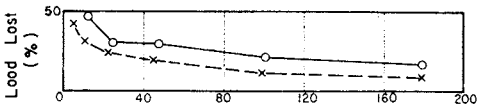
Fig. 2. Arrangement of lead markers in triaxial samples.

BALASUBRAMANIAM

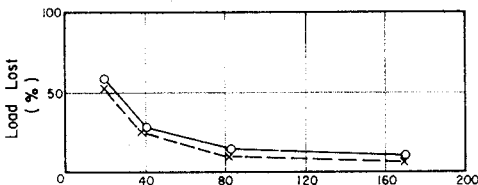
ONE DIMENSIONAL CONSOLIDATION TESTS WITH LEAD SHOT TECHNIQUE FOR THE MEASUREMENT OF LOCAL STRAINS

The structure of clay particles is assumed to have no preferred orientation after remoulding. However such orientation may develop during subsequent consolidation. HVORSLEV (1960) suggested that during the uniaxial consolidation of a remoulded clay that the particles developed a preferred orientation in a direction perpendicular to that of the major principal stress. THOMPSON (1962) suggested that this preferred orientation did not develop to the same extent simultaneously throughout any such sample, but he did not measure local strains within his samples. SIRWAN (1965) using the lead shot technique to measure local strains in consolidometer samples observed that the consolidation during the first application of load was larger in layers close to the free draining surfaces than for the other layers in the samples. For subsequent load increments he observed that the consolidation was larger in layers which were remote from the free draining surfaces than for those that were close. It must be emphasised that the mechanism of one dimensional consolidation is further complicated by the effects of side friction. Side friction measurements in consolidometers have been carried out by LEONARDS & GIRAULT (1961), THOMPSON (1962) and BURLAND (1967) among others. These measurements indicate that the magnitude of side wall friction can be reduced to a very small order by lubricating the walls with silicone grease. The one dimensional consolidation experimental results will be

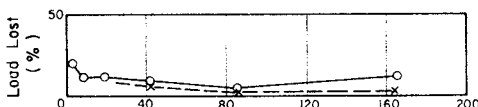
presented in the following sections. In addition to the strains the magnitude of side friction was measured by making use of a load cell at the base of the sample.



(a) Perspex Consolidometer



(b) Duralumin Consolidometer



(c) Triaxial Former with Rubber Lining

Fig. 3. Friction loss in consolidometers.

LOCAL STRAINS DURING CONSOLIDATION

lost in friction immediately after applying a load increment. The full lines refer to conditions two days after applying an increment. It is evident that the side friction was a minimum in the triaxial former which was lined with a rubber membrane.

Equilibrium Voids Ratio (e) vs. \log (stress σ) Plot for One Dimensional Consolidation

In Fig. 4 the full lines give the observed relationship between the equilibrium voids ratio (as measured from the final moisture content and the measured heights of the sample and the logarithm of the axial stress as calculated from the piston load. The dashed curves show the same relationship but now the stress is as recorded by the load cell at the base of the sample. The full lines have a slope $C_c = 0.31$, while for the dashed lines $C_c = 0.29$. For both types of swelling curves, their slopes k were approximately identical and equal to 0.045. The value of $C_c = 0.29$ may be compared to that of 0.25-0.26 obtained during isotropic consolidation in conventional triaxial specimens.

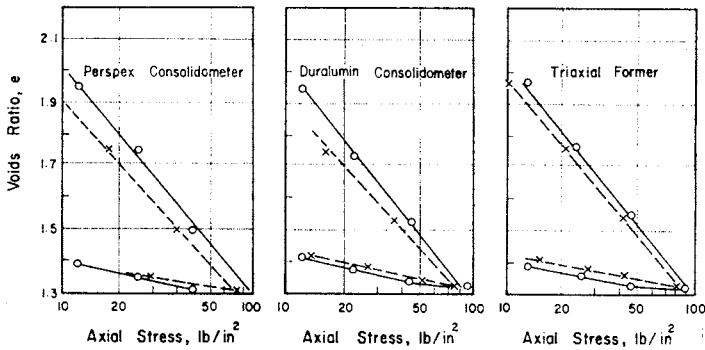


Fig. 4. Voids ratio-log pressure plot for one dimensional consolidation.

Variation of Consolidation with Depth during One Dimensional Consolidation

(i) *Consolidation during the first increment of stress:* Figure 5 illustrates the vertical displacement y of lead shot markers with respect to their vertical coordinates y as measured from the impermeable boundary of the sample. The three different symbols in this diagram refer to three different vertical columns or markers within the sample. It is evident that the sample was uniformly deforming since the displacement of all markers were linearly proportional to their initial vertical coordinates, for this first stress increment of 3 lb/in². During this increment of stress the clay, in the form of a slurry at 157% moisture content, was consolidated from a height of 8.5 inches to

BALASUBRAMANIAM

about 5.7 inches. The corresponding cumulative vertical strain being approximately 33%. In Fig. 5 the topmost layer of lead shot markers is about 0.7 inches below the free draining surface. Since no markers were arranged along this surface, the consolidation in the element of clay closest to it (which is about 0.7 inch thick) cannot be included in Fig. 5. Similar lead shot measurements carried out by SIRWAN (1965) during one dimensional consolidation of a slurry with an initial stress increment of only 0.26 lb/in², indicated that the consolidation in layers closest to the free draining surface is higher than the rest of the sample for this increment of stress.

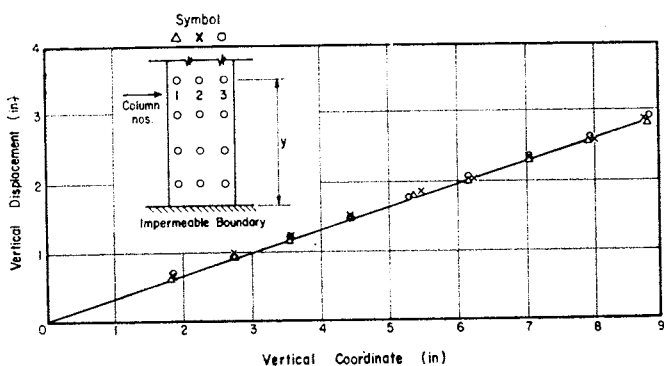


Fig. 5. Incremental vertical displacement of markers for first increment of stress during one dimensional consolidation from slurry.

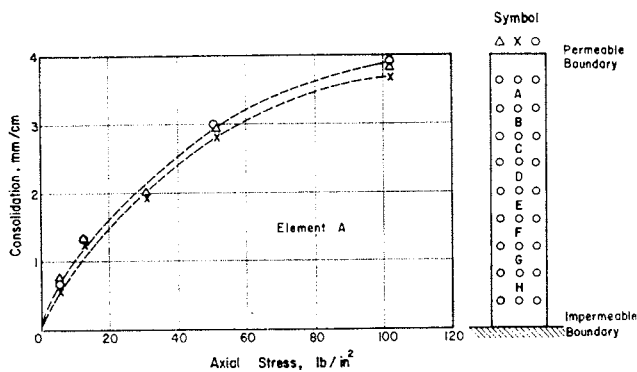


Fig. 6. Consolidation of 3 vertical columns in element A plotted with respect to the major principal effective stress.

(ii) *Consolidation during Subsequent Increment of Stress* : The subsequent stress increments were applied with a stress increment ratio of one, up to a maximum stress of 102 lb/in². Figures 6 to 8 show the variation of consolidation in mm/cm with the major principal stress for three horizontal elements A, D, and H at depths close to the free draining surface (element A), the mid height of specimen (element D) and the impermeable boundary (element H). It is observed in Figs. 6 to 8 that the consolidation of any hori-

LOCAL STRAINS DURING CONSOLIDATION

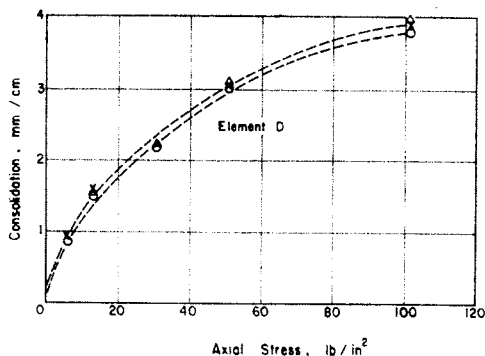


Fig. 7. Consolidation of 3 vertical columns in element D plotted with respect to the major principal effective stress.

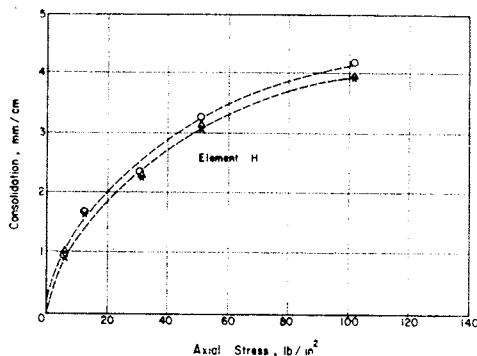


Fig. 8. Consolidation of 3 vertical columns in element H plotted with respect to major principal stress.

zontal element was uniform over its three vertical columns up to the maximum consolidation stress of 100 lb/in². Also in Fig. 9, the element A which was closest to the free draining surface had the least consolidation. The greatest consolidation was observed on the element H which was closest to the impermeable boundary. Element D which was approximately at mid section had roughly the average value of the consolidation of elements A and H. A similar phenomenon was observed by SIRWAN (1965) during increments subsequent to the first.

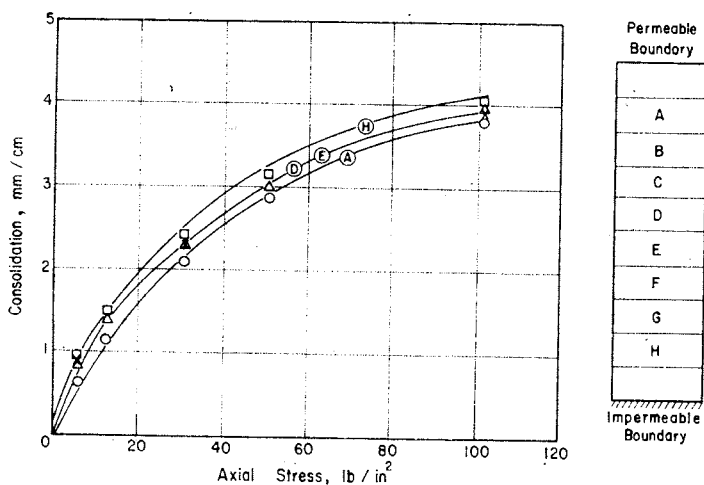


Fig. 9. Consolidation of 4 elements A, D, E and H plotted with respect to the major principal stress.

Comparison of the Average Overall Voids Ratio from Boundary Measurements with the Overall Average of the Local Values as Computed from the Lead Shot Measurement

The overall average voids ratio at the end of each increment of stress was computed from the final moisture content and the change in height of the

sample. Using the overall average voids ratio thus computed at the end of the first increment of stress subsequent local voids ratios were calculated from the displacements of the lead markers. When doing this the specimen was divided into eight horizontal sections A to H and the voids ratio of each element was calculated from its axial strain. Fig. 10 illustrates the variation of voids ratio from boundary measurements with respect to those computed from the average of the local voids ratio for the range of stress 0-100 lb/in². The excellent agreement between the two values indicates the power of the lead shot technique for the measurement of strains and voids ratios in clay specimens.

Variation of Voids Ratio with Time during a Stress Increment

The axial strain within each element (A-H) at specific intervals of time after the application of a stress increment was computed from the displacement of

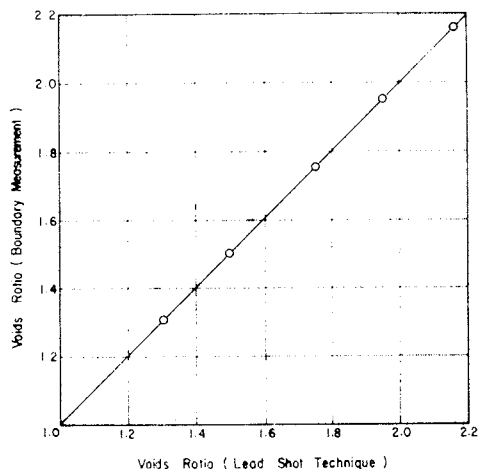


Fig. 10. Comparison of overall average voids ratio computed from the local measurements and the average overall voids ratio determined from the moisture content and change in heights of the sample.

the lead markers. The corresponding local voids ratios were determined from these strains. Using the Modified Theory of consolidation of DAVIS & RAYMOND (1965), the local voids ratio change with time at different depths in the specimen was calculated by the numerical method reported by RICHART (1957) from his equation 43. The experimental observations and the theoretical predictions are compared in Figs. 11 and 12. The local voids ratios computed from the displacements of the lead markers are in good agreement with the theoretical predictions for the top half of the sample. However for elements far from the free draining surface ($z/H > 0.6$: see Fig. 11) the experi-

mental observations are found to deviate from the theoretical predictions. These deviations may in part be due to the effects of secondary consolidation occurring simultaneously with the primary consolidation. Such a model incorporating primary and secondary consolidation is described by BRINCH HANSEN (1961).

LOCAL STRAINS DURING CONSOLIDATION

PORE PRESSURE ISOCHRONES AS DETERMINED FROM THE LOCAL VOIDS RATIO

The local effective stresses were calculated from the local voids ratio, using the logarithmic relationship between the voids ratio and the major principal effective stress shown in Fig. 4. The local pore pressures in the elements were then determined from the applied total stress and the calculated effective stress. Figures 13 (a) and (b) illustrate the pore pressure isochrones determined in this way with the curves drawn through the mean points. These isochrones are similar in form to those observed by actual local pore pressure measurements by BURLAND (1967) during one dimensional consolidation in a large consolidometer.

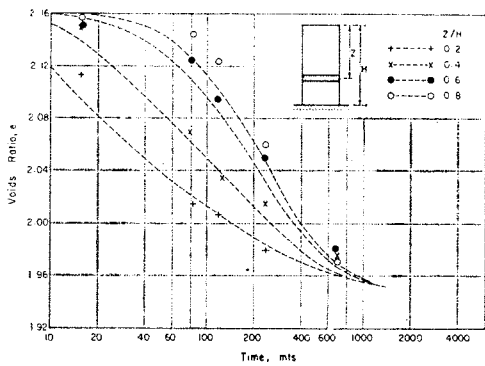


Fig. 11. Comparison of local voids ratios and the theoretical voids ratios at different depths during pore pressure dissipation for stress increment of 6 to 12 psi.

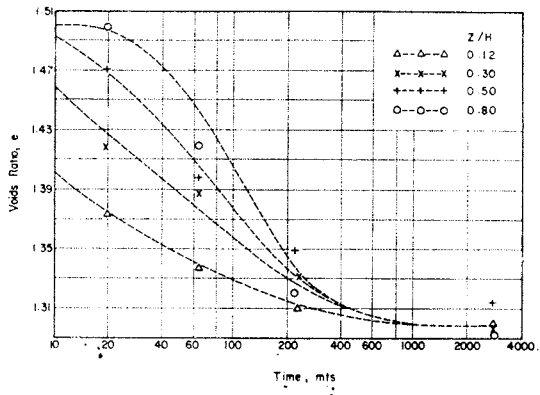


Fig. 12. Comparison of local voids ratios and the theoretical voids ratios at different depths during pore pressure dissipation for stress increment of 51 to 102 psi.

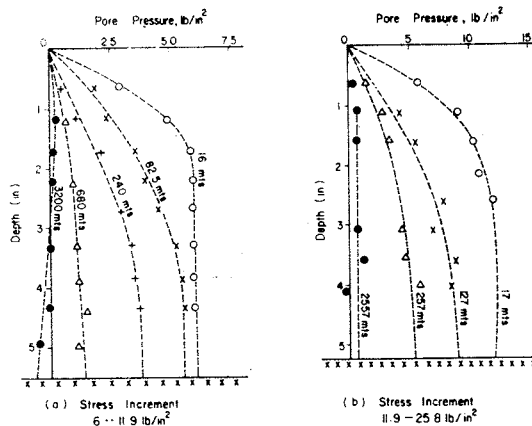


Fig. 13. Pore pressure isochrones determined from the local (a-b) measurements of voids ratios for two stress increments.

BALASUBRAMANIAM

ISOTROPIC CONSOLIDATION AND SWELLING USING LEAD SHOT
TECHNIQUE FOR STRAIN MEASUREMENT

In the investigation discussed in this section, specimens of kaolin initially prepared by one dimensional consolidation were subsequently further consolidated in the triaxial apparatus under isotropic stress conditions. The patterns of the axial and radial strain distributions during this isotropic consolidation were studied in detail for 1.5 inch diameter and the 4 inch diameter triaxial samples.

Effect of End Restraint on the Local Strains during Isotropic Consolidation of 1.5 inch Diameter \times 3 inch High Samples

Figures 14 (a) to (d) show the distribution along the axis of a 1.5 inch diameter sample, of the local (a) axial, (b) radial, (c) volumetric and (d) shear strains respectively that occur during the application of three successive increments of isotropic stress, the sample was contained between conventional friction type ends. In these figures it was observed for each increment of stress that

- (i) the axial strain was lowest at the top of the specimen and increased towards the bottom and
- (ii) the radial strain was a maximum at the top and a minimum at the base.

These distribution of strains are as to be expected if significant friction is present on the ends of the sample. A large porous stone (type UNI 150 kV) of 1.5 inch diameter was used at the base of the specimen. The effect of friction due to the porous rough surface was to reduce the lateral movement of the sample at the base and thereby decrease the radial strain. Fig. 14 (c) shows that the volumetric strain was virtually uniform throughout the sample. Hence the consolidation due to the isotropic stress increment is also uniform throughout the sample despite the observed nonuniformities of axial and radial strains. From Fig. 14 (d) it can be seen that the shear strain varies from -2 to $+3\%$ within the specimen. This may be due to the development of local anisotropy within the sample and will be discussed further. Figures 15 (a) to (d) refer to a similar series of tests to those discussed for Figs. 14 (a) to (d) but instead of frictional conventional ends the samples had lubricated conventional ends. Conventional lubricated ends were provided by replacing the porous stone used in the rough end by a $3/16$ inch thick highly polished brass disc covered with a thin layer of silicone grease. The strains throughout the samples with these lubricated ends were far more uniform than those with frictional ends.

LOCAL STRAINS DURING CONSOLIDATION

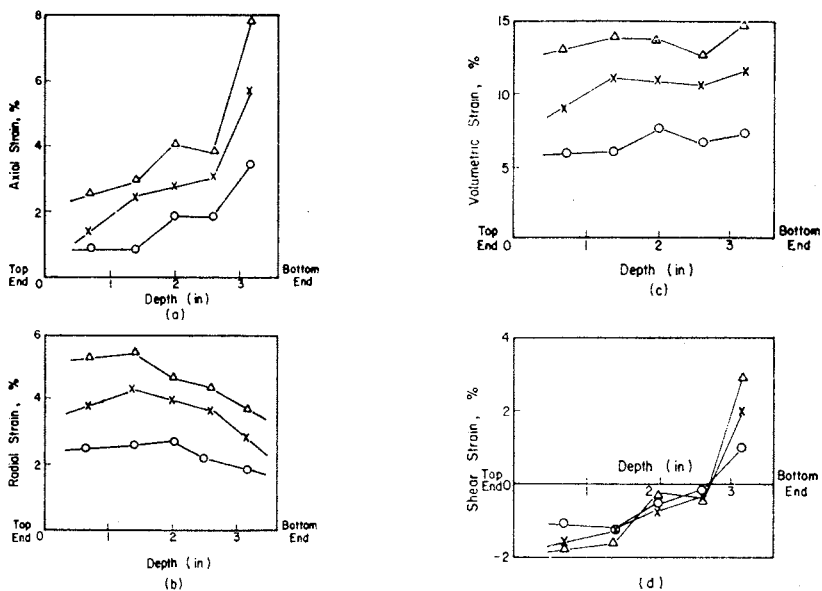


Fig. 14. Strain distributions plotted against the height of the sample (a-d) during isotropic consolidation (conventional frictional ends).

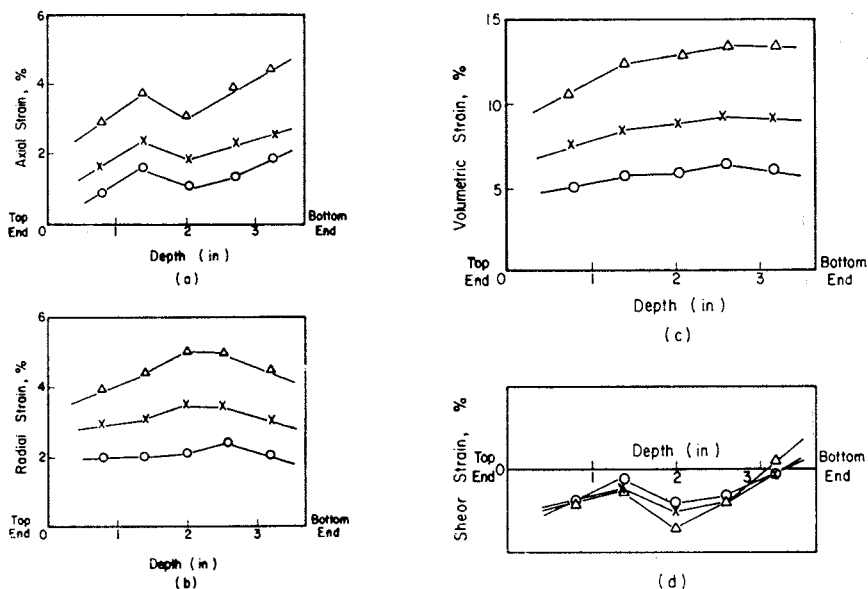


Fig. 15. Strain distributions plotted against the height of the sample during (a-d) isotropic consolidation (conventional lubricated ends).

BALASUBRAMANIAM

Distribution of Vertical and Horizontal Displacements of Lead Markers during Isotropic Consolidation in a 4 inch Diameter × 4 inch High Sample

In the previous section it was noted that the lubricated end condition produces more uniform strains during isotropic consolidation than the rough end condition. A detailed investigation of the radial and axial displacements of the lead markers in two perpendicular vertical planes passing through the axis of the specimen was then carried out in a 4 inch diameter triaxial sample. The objective was two-fold in that

- (i) the radial strain distribution cannot be studied in detail with the 1.5 inch diameter sample and
- (ii) any effect of the increase in length of drainage paths due to the small porous stones which were used with the lubricated ends should show up markedly in a larger sample.

The markers were arranged in two perpendicular planes as illustrated in Figs. 16 and 17. The vertical displacement patterns with respect to height within the sample and the horizontal displacement patterns at different radii within the sample are shown in Figs. 18 and 19. The remarkably linear variations of the displacement patterns indicate that both the axial and radial strains are uniform. Similar results are obtained from the displacement of the lead markers in the perpendicular plane. Therefore the assumption $\epsilon_2 = \epsilon_3$ made in the calculations of strains in triaxial specimens is justified.

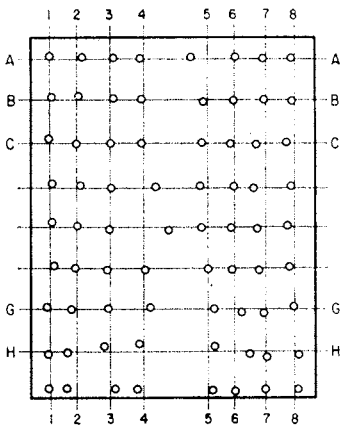


Fig. 16. Positions of lead markers in plane 1 of 4 inch diameter sample.

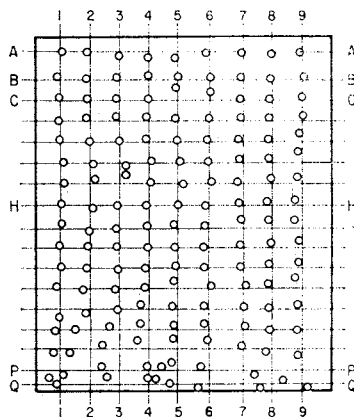


Fig. 17. Positions of lead marker in plane 2 of 4 inch diameter sample.

Effect of Anisotropy on the Axial and Radial Strains during Consolidation under Isotropic Stress

It has already been stated that all the specimens were initially prepared under one dimensional consolidation conditions. Hence all specimens were

LOCAL STRAINS DURING CONSOLIDATION

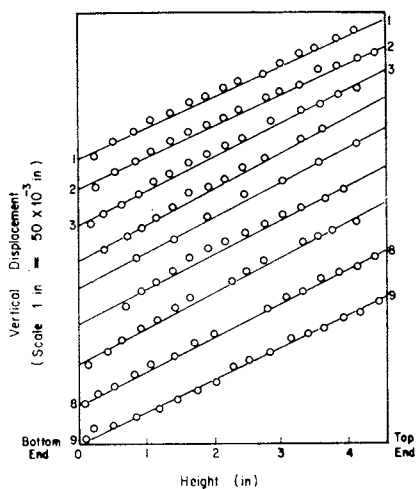


Fig. 18. Incremental vertical displacements of markers plotted against the height of the markers above the base for nine vertical columns in plane 2 of 4 inch diameter sample during isotropic consolidation.

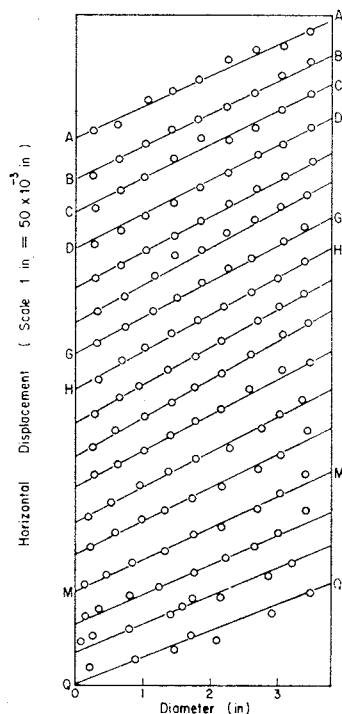


Fig. 19. Incremental horizontal displacement of markers plotted against their distances along the diameter for seventeen horizontal rows in plane 2 during isotropic consolidation.

subjected to an initial shearing process. The subsequent application of increasing isotropic stress gradually erases the effect of the initial one dimensional consolidation. This is best illustrated in Fig. 15 (d) where it is observed that during the application of the first increment of isotropic stress, a shear strain with a maximum value of 1% is observed. Subsequent increase in isotropic stresses do not produce any further increase in the shear strain, indicating that the strains due to these increments of stress are isotropic. The data suggests that specimens isotropically consolidated to approximately three times the initial one dimensional stress can be assumed to have lost their previous shear stress history effects. A similar observation was also noted by LOUDON (1967) using a different technique for the strain measurement.

Slopes of the Isotropic Consolidation Lines in the (e , $\log p$) Plot for Overall Voids Ratio as Determined from the Average Local Voids Ratio

The average volumetric strain in the sample during an increment of isotropic stress was determined from the local measurements of strains. The

BALASUBRAMANIAM

overall voids ratio at the end of each increment was obtained from the final overall average voids ratio of the sample (obtained from the final moisture content determination) and the average volumetric strains computed from the lead shot measurements. Figs. 20 (a) and (b) illustrate the variation of these voids ratio with $\log p$ for tests carried out with the two types of end conditions discussed before. These relationships are linear in the $(e, \log p)$ plot with the slope λ varying from 0.25 to 0.26. This value of λ is extensively used in the Stress Strain Theories developed at Cambridge (see ROSCOE et al (1963), ROSCOE & BURLAND (1968) and hence the lead shot technique offers a mean by which this value of λ could be assessed independently. Conventionally the value of λ is determined from isotropic consolidation tests and on the assessment of the change in voids ratio as indicated by the change in volume of water in a burette connected to the base of the specimen. The leakage of cell fluid into the specimen and the leakage of water from the specimen and from the drainage connections could thus cause an error in the assessment of λ from the volumetric measurements as made from the burette readings.

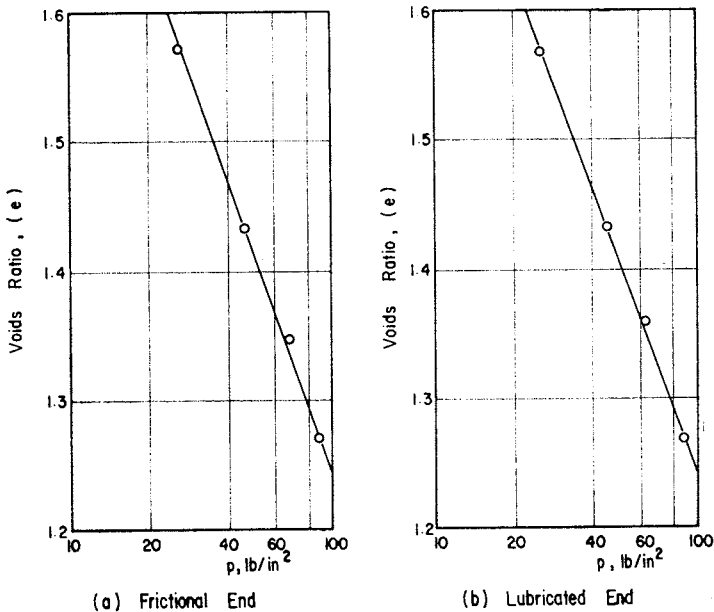


Fig. 20. Voids ratio-log. pressure plot during isotropic consolidation.

Distribution of Vertical and Horizontal Displacements of the Lead Markers during Isotropic Swelling

Figures 21 and 22 illustrate the vertical and horizontal displacements of the lead markers during isotropic swelling. The displacements are seen to be linear. Similar linear displacement patterns are noted in the orthogonal plane. However the slopes of the lines corresponding to the horizontal displacements

LOCAL STRAINS DURING CONSOLIDATION

at the bottom end of the sample are considerably less than for the other lines. Hence the radial strains at the bottom end of the sample were lower than in the rest of the sample. This reduction in strain was in part due to errors in measurement as the markers were placed extremely close to the cell pedestal and the scattered radiation from this pedestal tended to blur the images of the markers in the radiograph, thereby reducing the contrast and definition of these images. The average axial and radial strains as determined from the mean slopes of the lines during swelling under isotropic stress are -2.66 and -1.34% respectively. These results indicate that the strains were anisotropic during swelling under isotropic stress conditions. A similar phenomenon was also observed by BURLAND (1967) during isotropic swelling using a different technique for the measurement of strains.

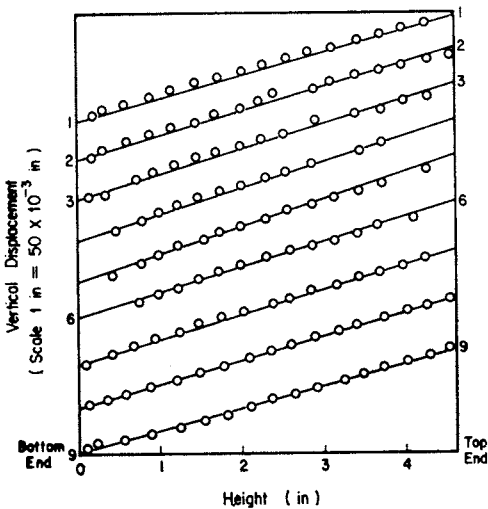


Fig. 21. Incremental vertical displacements of lead markers plotted against their heights above base for nine vertical columns in plane 2 of 4 inch diameter sample during isotropic swelling.

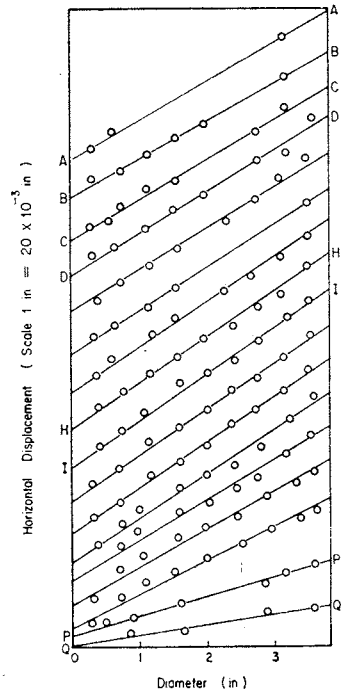


Fig. 22. Incremental horizontal displacements of lead markers plotted against their distances along the diameter for 17 horizontal rows in plane 2 of 4 inch diameter sample during isotropic swelling.

CONCLUSIONS

- (1) The friction measurements carried out during one dimensional consolidation indicates that the percentage load lost in friction can be reduced

BALASUBRAMANIAM

to as low as 10% by lining the inner surface of the consolidometer with a rubber membrane lubricated with a thin layer of silicone grease.

- (2) The local measurements of strains carried out with the lead shot technique show that the consolidation was uniform throughout the sample for the first increment of stress, when the clay (initially in the form of a slurry 160% moisture content) was consolidated to about two-thirds of its original height. For subsequent stress increments, elements of clay nearest to the free draining surface were found to experience less consolidation than elements further from it.
- (3) The change of overall voids ratio as computed by summing the local values obtained from the local measurements of strains were in excellent agreement with those determined directly from the boundary measurements at all stress levels.
- (4) The observed local voids ratio changes with time when compared with the corresponding theoretical values as derived from the Modified Theory of DAVIS & RAYMOND (1965) using the numerical procedure of RICHART (1957) illustrate (a) the observed local voids ratio was in good agreement with the theoretical predictions for the top half of the specimen which was close to the free draining surface (b) for elements far from the free draining surface the experimental observations deviated from the theoretical predictions.

The pore pressure isochrones determined from the local measurements of voids ratio were similar to those observed by actual local pore pressure measurements by BURLAND (1967).

- (5) For specimens contained between frictional ends, the axial and radial strains were found to be nonuniform during isotropic consolidation. With the use of lubricated ends this nonuniformity in strains was reduced to a minimum. In both specimens the local volumetric strains were observed to be uniform throughout the sample.
- (6) For isotropic stresses of similar magnitude to the initial one dimensional stress, the strains induced by increments of isotropic stresses were found to be anisotropic. However for specimens which were isotropically consolidated to approximately three times the initial one dimensional stress, the effect of anisotropy was found to be small.
- (7) Experiments performed on 4 inch diameter samples showed that the axial and radial strains were uniform but not equal during swelling under isotropic stresses.

LOCAL STRAINS DURING CONSOLIDATION

ACKNOWLEDGEMENTS

The work presented in this paper was carried out at the Engineering Laboratories, University of Cambridge while the Author was a research student. The author wishes to thank his supervisor Dr. R.G. James and the late Prof. K.H. Roscoe for their invaluable guidance and unstinted help. The manuscript of this paper was prepared at the Faculty of Engineering, University of Ceylon, Peradeniya, Ceylon. Thanks are due to Prof. A. Thuraiajah for his continuous support and encouragement.

REFERENCES

- BALASUBRAMANIAM, A.S. (1969), Some Factors Influencing the Stress Strain Behaviour of Clays, *Ph.D. Thesis, Cambridge University*.
- BURLAND, J.B. (1967), Deformation of Soft Clay, *Ph.D. Thesis, Cambridge University*.
- BURLAND, J.B. and K.H. ROSCOE (1969). Local Strains and Pore Pressures in a Normally Consolidated Clay Layer during One Dimensional Consolidation, *Geotechnique*, Vol. 19, pp. 335-356.
- DAVIS, E.H. and G.P. RAYMOND (1965), A Non-linear Theory of Consolidation, *Geotechnique*, Vol. 15, pp. 161-173.
- HANSEN, J.B. (1961), A Model Law for Simultaneous Primary and Secondary Consolidation, *Proc. 5th Int. Conf. on Soil Mech. and Found. Eng.*, Vol 1, pp. 133-136.
- HVORSLEV, M.J. (1960), Physical Component of the Shear Strength of Saturated Clays, *Research Conf. on Shear Strength of Cohesive Soils*, ASCE, pp. 169-273.
- JAMES, R.G. (1965), Stress and Strain Fields in Sand, *Ph. D. Thesis, Cambridge University*
- LEONARDS, G.A. and P. GIRAULT (1961), A Study of the One Dimensional Consolidation Test, *Proc. 5th Int. Conf. Soil Mech. and Found. Eng.*, Vol. 1, pp. 213-218.
- LORD, J.A. (1969), Stresses and Strains in an Earth Pressure Problem, *Ph.D. Thesis, Cambridge University*.
- LOUDON, P.A. (1967), Some Deformation Characteristics of Kaolin, *Ph.D. Thesis, Cambridge University*.
- RICHART, F.E. (1957), A Review of the Theories for Sand Drains, *Proc. ASCE*, 83.3.1957 pp. 1301-1338.
- ROSCOE, K.H., J.R.F. ARTHUR and R.G. JAMES (1963), The Determination of Strains in Soils by an X-ray Method, *Civ. Eng. and Pub. Wks. Rev.*, Vol. 58, pp. 873-876 and 1009-1012.
- ROSCOE, K.H. and J.B. BURLAND (1968), On the Generalised Stress Strain Behaviour of Wet Clay, *Engineering Plasticity, Cambridge University Press*, pp. 535-609.
- ROSCOE, K.H., A.N. SCHOFIELD and A. THURAIRAJAH (1963), Yielding of Clays in States Wetter than Critical, *Geotechnique*, Vol. 13, pp. 211-240.
- SIRWAN, K.Z. (1965), Deformation of Soil Specimens, *Ph.D. Thesis, Cambridge University*.
- THOMPSON, W.J. (1962), Some Deformation Characteristics of Cambridge Gault Clay, *Ph. D. Thesis, Cambridge University*.
- THURAIRAJAH, A. (1961), Some Shear Properties of Kaolin and of Sand, *Ph.D. Thesis, Cambridge University*.

LONG PILES UNDER TENSILE LOADS IN SAND

R.H.S. TAN* and T.H. HANNA[†]

SYNOPSIS

The relationships between initial residual stress state along the length of a pile and volume change effects near to the pile walls are studied experimentally for piles in tension. It is shown that the mechanism of load development is not in agreement with any of the standard bearing capacity theories but agrees with concepts presented earlier by the authors. Data are given for piles of length/diameter ratio up to 110 as well as for piles with bells spaced along the length of the shaft.

INTRODUCTION

The state of stress in a soil mass is usually denoted by a vertical effective stress, $\bar{\sigma}_v$, and a horizontal effective stress, $\bar{\sigma}_H$, at any point, the ratio of $\bar{\sigma}_H/\bar{\sigma}_v$ being the coefficient of earth pressure at rest, K_0 . It is well established that the values of K_0 depend on the soil type and the geological loading history of the soil stratum. For normally and lightly overconsolidated soils $K_0 < 1$ while for heavily overconsolidated soils $K_0 > 1$.

When a pile is placed in such a soil deposit either by a driving technique or a cast-in-situ method, the stress state in the soil near to the pile is altered in a complex manner. The practising engineer has allowed for these stress changes by the introduction of empirical coefficients such as undrained strength modification factors, α , to give adhesion on piles in clay (SKEMPTON, 1959), or by the use of empirical earth pressure coefficients in sand (MEYERHOF, 1963).

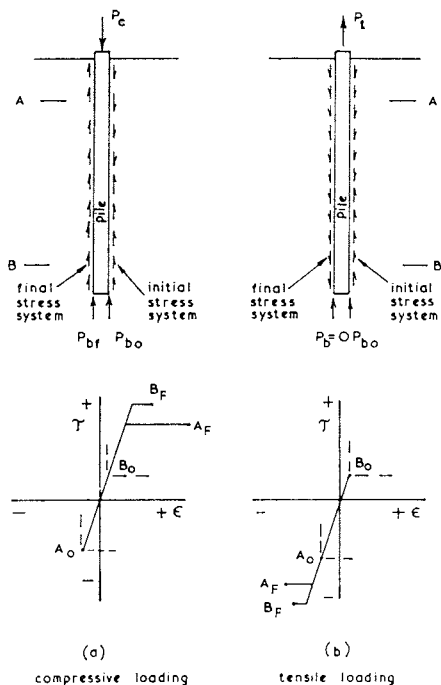
In addition to the stress changes which occur in the soil mass near to a pile, the pile installation or construction process induces relative displacements between the pile member and the adjacent soil. Consequently the pile shaft is not stress free prior to the application of an external load but it is in equilibrium under an initial residual stress system. The general mechanics of this phenomenon have been worked out by HANNA (1969, 1971) for vertical piles while the particular case of inclined anchor piles in clay soils has been examined in a tentative manner (HANNA, 1973).

With relatively short piles the importance of the initial residual stress system is not very large but with very long piles such as those in use for

* Civil Engineer, University of Singapore.

[†] Professor of Civil and Structural Engineering, University of Sheffield, U.K.

Discussion on this paper is open until 1 May, 1975.



IDEAL STRESS STRAIN REPRESENTATION OF ELEMENTS A & B

Fig. 1. Representation of the stress and strain state acting on typical small elements A and of the soil/pile interface.

and to support these general concepts by the results of several series of laboratory experiments.

IDEALIZATION OF PILE MECHANICS

As explained by HANNA & TAN (1971), an unloaded pile must be under a system of internal stresses and Fig. 1 shows the origins of the stress/strain relationships of typical elements A and B starting, not at 0, but at unknown points A_o and B_o . When a pile is load tested the recorded overall behaviour will depend on the vectorial sum of the behaviours of the individual elements such as A and B along the length of the pile. The general case of both compressive and tensile loading is idealized in Fig. 2. In these idealizations it has been assumed that arching phenomena, such as those discussed by VESIC (1969), do not occur. The primary significance of arching is to modify the strength of the typical elements A and B and consequently the general hypothesis of Hanna & Tan that the initial stress state in the vicinity of the pile member governs the shape and the magnitude of the subsequent loading diagram still holds. Consequently, the sequence of loading to which a pile has been subjected during or subsequent to installation in the ground will influence its

marine structures and in thick estuarine deposits the influence of initial residual stress becomes greater. Also there are design circumstances where the pile may experience a compressive load followed by tensile loading or vice-versa. The loading and subsequent unloading of a pile results in a residual stress system, different from the initial residual stress state, being locked in the pile. The significance of this is that the performance of that pile under subsequent loading will be regulated by the previous loading state.

The purpose of this paper is to present a general idealization of the mechanics of load transfer of piles subjected to pull-out

LONG PILES UNDER TENSILE LOADS

subsequent behaviour under static load. Further details of the general mechanics are given by HANNA & TAN (1971, 1973).

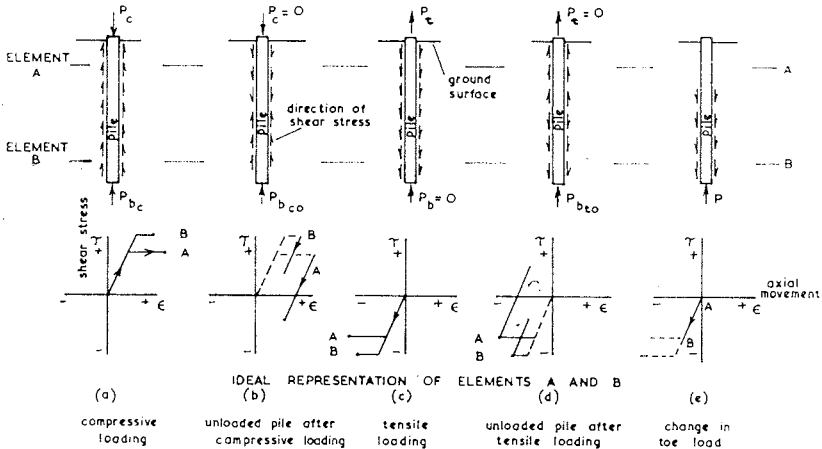


Fig. 2. Representation of soil/pile elements for a range of pile loading conditions.

TEST APPARATUS

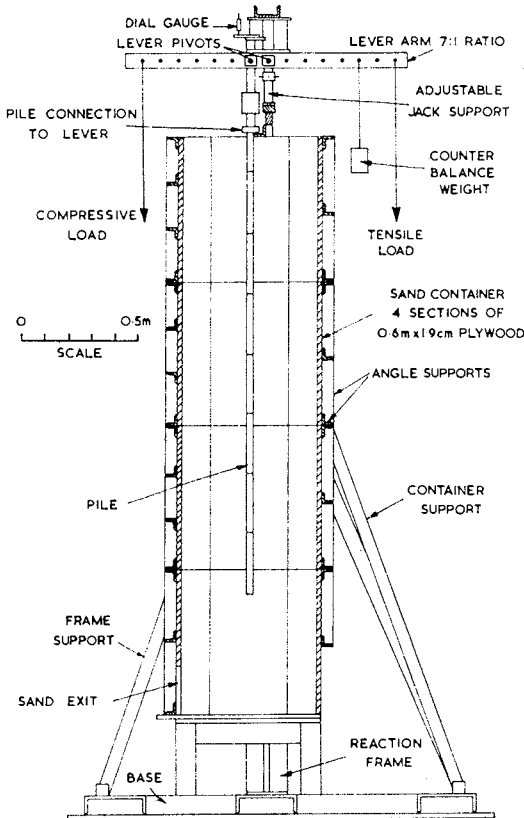


Fig. 3. The pile test apparatus.

General features of the test apparatus are given by HANNA & TAN (1973). It consists of a 0.6 m square by 2.4 m high flume, the test pile being suspended from a central loading lever (Fig. 3). The top end of the pile could be held rigid during sand preparation or it could float as the sand was placed around it. Thus it was possible to include any combination of tensile or compressive loading in the test programme. The sand medium was poured through a 75 mm diameter hose pipe held 250 mm above the sand surface, the sand flowing through a 6.5 mm wire mesh. The sand was well graded between sieve numbers 10 and 72, the average bulk density being 1.546 Mg/m^3 (relative density = 41%).

TAN AND HANNA

The piles were 1.8 m long aluminium alloy tubes with outside diameters in the range 15.9 to 38.1 mm., the pile wall thicknesses being between 3.3 and 0.49 mm. The piles were provided with load transducers in the form of a temperature compensated proving ring or a thin tube in tension. The load transducers could record both tensile and compressive forces and had a sensitivity of 60 μ strains per kg. Details of load cell design are given by TAN (1971).

With the method of load cell installation in the test piles it was possible to measure the force system along the length of the pile during and after sand placement and also at any stage of a loading test. Repeatability both with respect to total load and residual load was within 2 % in all cases.

TEST RESULTS

Residual Load due to Sand Filling

Figure 4 shows how axial load developed in a 25.4 mm diameter pile which was allowed to float as the sand bed was formed around it. With depth of sand fill increase compressive loads were developed in the pile. Peak compressive loads were recorded and the position of these peak values is referred to as the neutral point. The location of the neutral point changed with sand placement. As the sand was placed around the pile the top of the pile settled (Fig. 4 b). Depending on the displacement of the pile relative to the soil a system of negative or positive shear stresses is developed along the length of

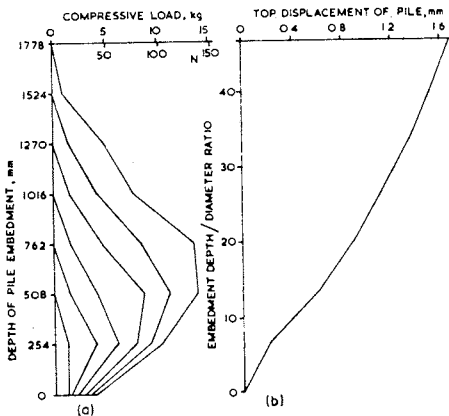


Fig. 4. (a) Development of compressive loads in a pile during sand placement.
 (b) Development of pile top movement during sand filling.

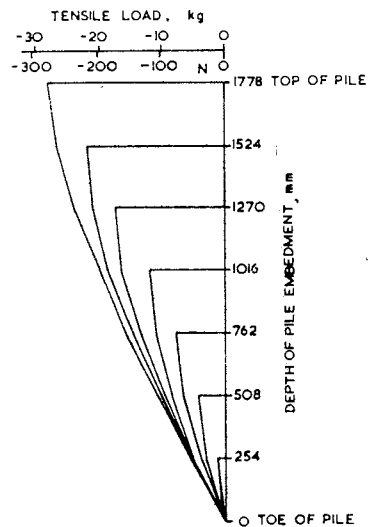


Fig. 5. Development of tensile load in "held" pile during sand filling around the pile.

LONG PILES UNDER TENSILE LOADS

the pile. The neutral point occurs where there is no relative displacement between the pile and the sand. Below the neutral point positive shear stresses develop while above it negative shear stresses occur. At any stage of sand bed preparation the sum of the residual shear stresses on the pile shaft is equal to the pile tip load.

By restraining the top end of the pile from moving during sand placement (held pile), the displacement of the sand was relative to the pile and thus a negative shear stress was created along the length of the pile as shown in Fig. 5. No pile tip load was recorded, the sum of the negative shear stresses being equal to the tensile force at the top end of the pile.

These very simple and idealized pile construction techniques illustrate the significant control which they have on the initial residual force system in the pile and, as discussed in the next section, these residual forces can have a major influence on the subsequent loading behaviour of the pile.

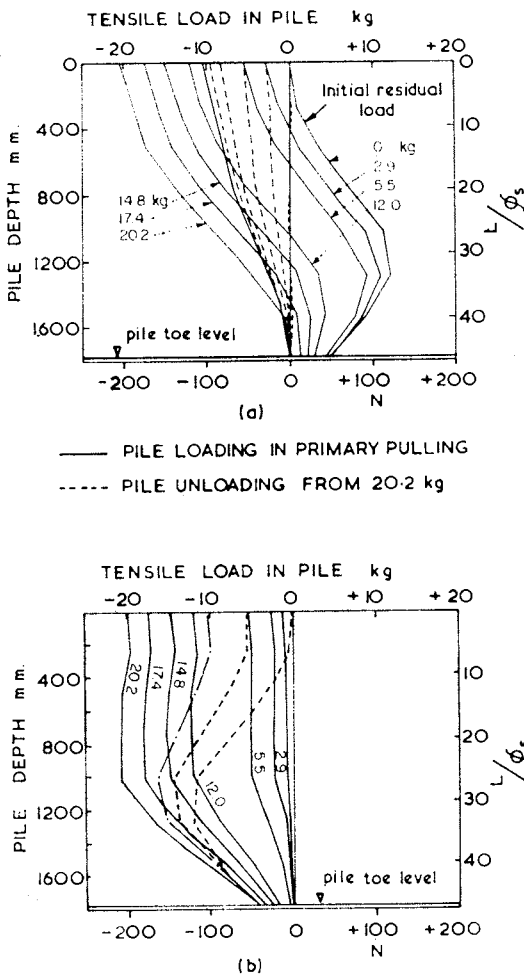


Fig. 6. Distribution of axial load in a 25.4 mm diameter "floating" pile.
 (a) allowing for initial residual load distribution,
 (b) neglecting initial residual load distribution.

Tensile Tests

The distribution of axial load in a 25.4 mm diameter pile is shown in Fig. 6. When the pile was loaded to 2.9 kg in tension, no load change was caused at the pile tip. This load decreased the positive shear stress along the lower part of the pile. Note that below a depth of 400 mm the pile was in compression. Increase of the tensile load to 5.5 kg caused a transfer to negative shear along the length of the pile with a decrease in the initial residual toe load value. As the applied tensile load was increased, negative shear stresses along the pile length were progressively mobilized and at failure the toe load value was zero. When the pile was unloaded in increments load flowed

out of the top of the pile and at zero applied external load the residual load left in the pile is shown by the dashed line in Fig. 6 (a).

The test data for this pile are also shown plotted in Fig. 6 (b) in which no allowance has been made for the initial residual stress state existing in the pile. Several observations are pertinent. First, after unload the pile was virtually stress free (Fig. 6 a). Secondly, without allowance for initial residual load effects the pile appears to carry a large negative (tensile) axial toe load. Such an observation could lead to a very unreal analysis of the pile data. In the case of the pile which was held at the top end during the sand placement, a very small pile top movement of 0.03 mm occurred before failure. As mentioned earlier the tensile stresses along the length of the pile (Fig. 5) after the completion of the sand filling operation, were almost at their maximum values and consequently the pile was in a stress state near to failure. The ultimate pulling load for this pile was 28.3 kg which was 132% of the ultimate pulling load of the same pile (Fig. 6) which was allowed to float

during the sand placing operation.

Division of the difference in measured axial load between adjacent load transducers by the shaft surface area of the pile between these transducers, gave the average shear stress mobilized at the sand-pile interface. Figure 7 shows the measured average shear stresses for the pile which was allowed to "float" during the sand placing operation. The values shown alongside the shear stress curves are the applied top loads in kilogrammes. After the placing of the sand around the pile, the upper portion of the pile was subjected to a negative shear stress and the lower portion of the pile was under a positive shear stress with a positive pile toe load. The neutral point was at a depth of 1100 mm. On application of the pulling load, the negative shear stress along the upper portion of the pile increased slightly until it reached its

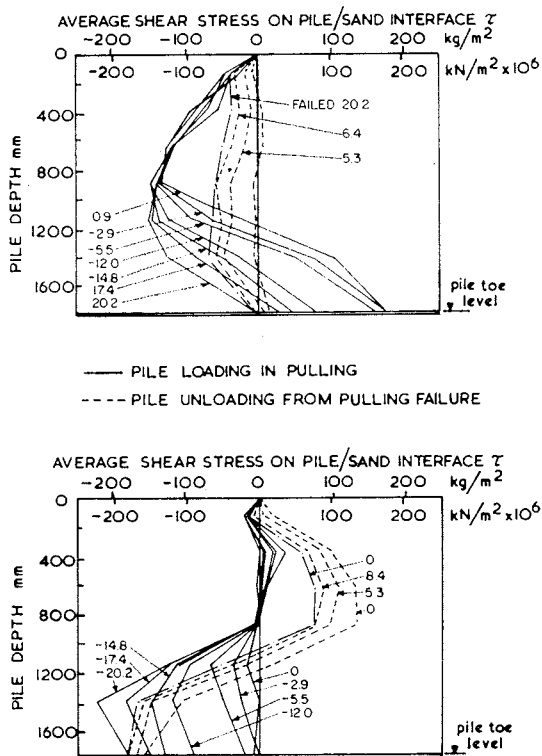


Fig. 7. Average shear stress on the sand-pile interface with applied load for a 25.4 mm diameter "floating" pile (a) allowing for initial residual stresses in the pile and (b) neglecting initial residual stresses in the pile.

LONG PILES UNDER TENSILE LOADS

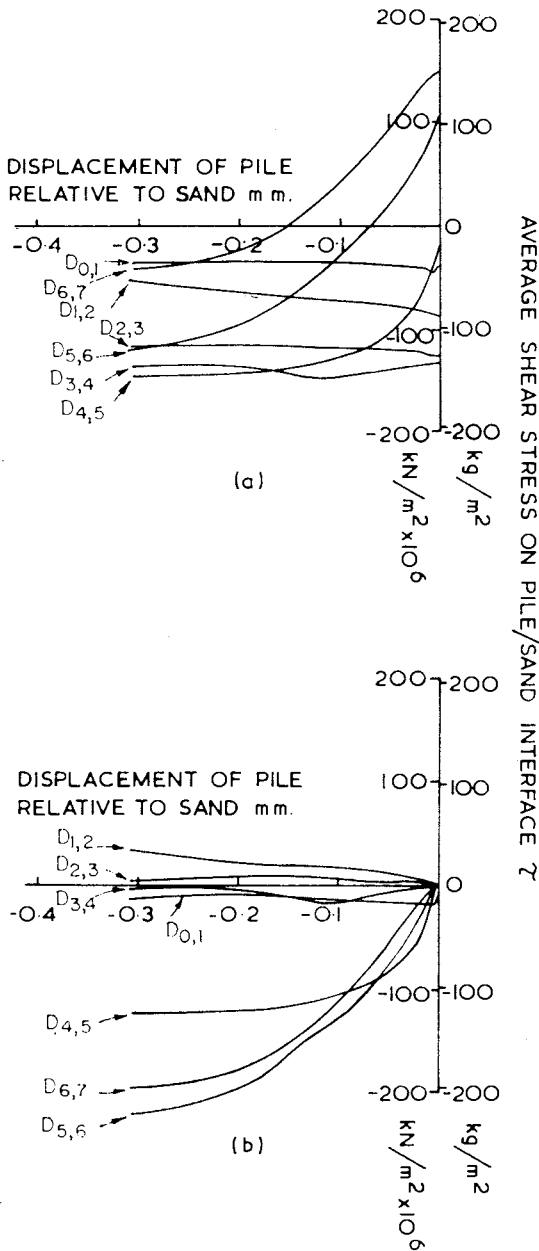


Fig. 8. Development of shear stress along the length of the pile with displacement — “floating” pile.

ultimate value and the positive shear stress in the lower parts of the pile decreased, the magnitude of the pile toe load also decreasing. Failure of the pile in pulling occurred when the maximum shear stress had been fully mobilized along the pile length. After unloading very small residual shear stresses remained in the pile. Comparison of Figs. 7 (a) & (b) shows the influence of the initial residual shear stress on the magnitude of the shear stress values mobilized.

By plotting curves of average shear stress against pile displacement as shown in Fig. 8 for a floating pile, the mobilization of shear stress with displacement was found. At very small relative displacement an approximately linear relationship between shear stress and displacement resulted. Along the top of the pile, where very large initial residual negative shear stresses existed, a limiting displacement of 0.01 mm caused failure while displacements between 0.1 and 0.25 mm were required to cause failure along the lower part of the pile. At displacements in excess of these values the average shear stress remained approximately constant in value. The magnitude of the maximum shear stress mobilized was not constant as

assumed in the conceptual models of HANNA & TAN (1971), but varied, the largest unit average shear stresses being in the mid-height region of the pile.

The idealized shear stress-relative displacement diagrams bear no resemblance to the true diagrams (Fig. 8 b). It will be noted that for the idealized test the maximum negative shear stress was 50% higher than the true value

and the maximum positive shear stress was only 23% of the true value.

Figure 8 showed that shear stress mobilization at the pile-sand interface depended on the relative displacement between the pile and the sand. Three piles of length 1778 mm, diameter 25.4 mm and wall thicknesses 3.33, 1.22 and 0.49 mm respectively were tested. All piles were allowed to float during sand bed preparation. It was found that at small displacements the stiffest pile required larger displacements for the same applied load than the more flexible piles. The ultimate pull-out loads were 14.7 kg, 14 kg and 11 kg in order of pile stiffness increase (Fig. 9). The increase in pull-out load with flexibility increase is due to the higher initial residual stresses locked in the pile during sand bed preparation. Also shown in the bottom of Fig. 9 are the axial compressions of the piles during sand bed preparation and the axial extensions during the pulling tests.

In the main test programme a large number of piles of different lengths and diameters was tested for the floating case and when the average shaft friction

resistance was plotted against depth (depth/diameter ratio), it was found that the unit resistance increased up to a depth diameter ratio of 40 and was practically constant beyond this depth (Fig. 10). This observation supports the general trend put forward by KERISEL & ADAM (1969) and VESIC (1955) that below a certain depth arching effects in the soil change the stress state in the vicinity of the pile and consequently the effective stress on the pile shaft does not increase linearly with depth.

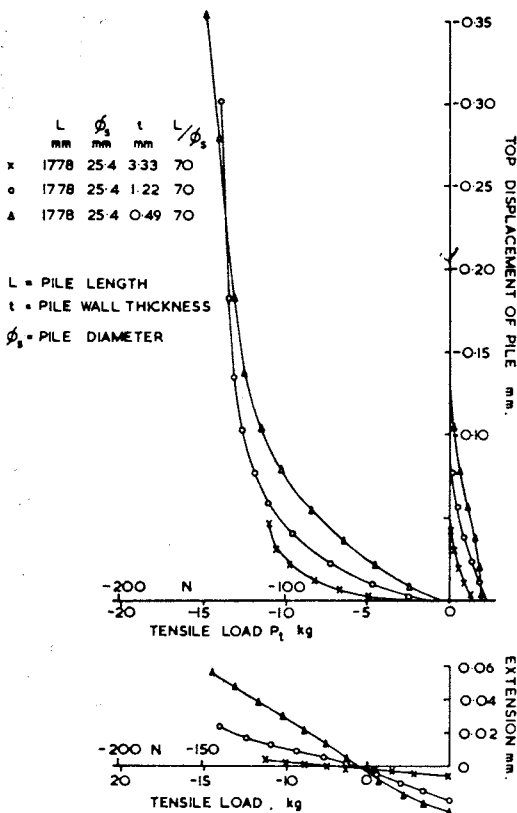


Fig. 9. Top load-top displacement diagrams for "floating" piles of different stiffness.

Effect of Pile Loading History on Pulling Resistance

It has been shown that the initial residual stress state along the length of a pile regulated the subsequent loading behaviour of that pile. Because in many situations piles

LONG PILES UNDER TENSILE LOADS

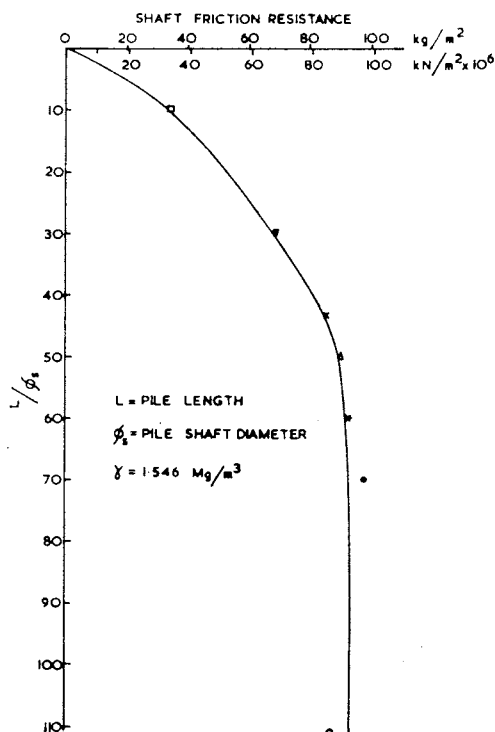


Fig. 10. Ultimate shaft friction resistance — depth of embedment / pile diameter ratio for “floating” piles.

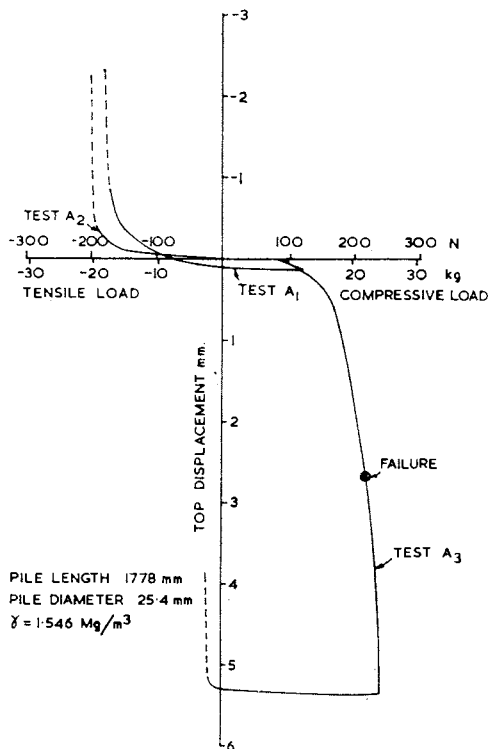


Fig. 11. Effect of test method on ultimate pulling resistance for a 25.4 mm diameter floating pile.

may be subjected to load reversals it was decided to apply a compressive load followed by a tensile load. Figure 11 shows the results of three load tests. Test A1 was a compressive load test carried to about 50% of the ultimate compressive load and 5% of the ultimate displacement. The pile was unloaded and then pulled to failure. In test A2 the same pile was initially pulled to failure. The ratio of the tensile ultimate loads in tests A1 and A2 was 0.89. In the third test the pile was initially pushed to failure (A3), unloaded and then pulled to failure. The ultimate pulling load in this case was only 10.6% of that for test A2 and 11.9% of that for test A1. This very simple test, therefore, shows the significance of mode of loading on ultimate carrying capacity.

Multi-Belled Pile Behaviour

To quantify the effect of placing a series of footings along the length of the pile shaft and at predetermined positions, footings of 50.8 mm diameter were placed at 254 mm intervals by the use of special fittings. The pile diameter was

25.4 mm. Figure 12 compares the top load-top displacement behaviour of the 25.4 mm diameter straight-sided comparator pile with the same pile but having footings attached at pile toe level and along the pile length. The loads taken by the base footing were found to be independent of the number of footings used, having an ultimate value of about 14 kg. With increase in the number of footings the shape of the load-movement curve changed, the movements required to cause failure increasing. Compared with the straight-shafted pile, an ultimate load increase of 8 times for the pile with seven footings was found. This observation suggests that the footings were acting with the adjacent pile sections as units and hence failure occurred not along a cylindrical surface of diameter equal to that of the footings but in a modified bearing failure at each footing projection. Figure 13 compares the performance of a straight-side pile of diameter 38.1 mm with a 25.4 mm pile with 7 equally spaced footings of 38.1 mm and 50.8 mm diameter, spaced at 254 mm centres. The failure load of the multi-belled pile was 66.5 kg at a displacement of 6.34 mm while the straight-sided pile carried 18.9 kg at failure, the corresponding displacement of this pile top was only 0.19 mm. These observations show the desirability for provision of a series of corrugations along the length of a pile. Similar conclusions have been put forward by MOHAN et al (1969) and HANNA & TAN (1973) for piles in bearing and by Mohan et al for piles in tension.

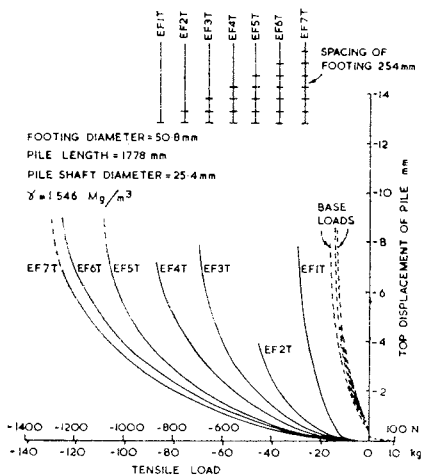


Fig. 12. Comparison of top load – top displacement diagram for a 25.4 mm diameter “floating” pile with 1 to 7, 50.8 mm diameter footings spaced along the pile at 254 mm centres.

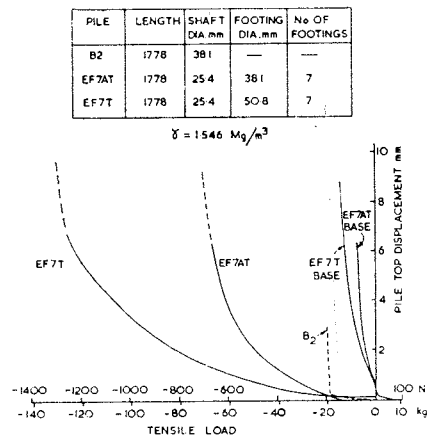


Fig. 13. Comparison of top load – top displacement diagrams for a 38.1 mm diameter pile with a 25.4 mm diameter pile with 7, 38.1 mm or 50.8 mm bells at 254 mm centres.

LONG PILES UNDER TENSILE LOADS

Comparison of Piles in Pulling and Pushing

The theoretical concepts put forward by HANNA & TAN (1971) suggested that the load carrying capacity of a pile in either tension or compression depends on (i) the initial stress state along the pile prior to loading and (ii) the sequence of loading followed. Because there are basic differences in the stress changes to which elements of the soil near to the pile surface are subjected during loading it would be expected that piles in tension will behave in a different manner to piles in compression. It has been argued and confirmed by test that the load carrying capacity of a pile is a function of the direction of shear along the pile shaft, the applied shear stress due to loading being added to the initial residual shear stress. Because of the presence of arching effects in the soil around the pile it is impossible to quantify the problem by engineering mechanics methods. Figures 14 and 15 show comparisons of compressive and tensile loading for a 25.4 mm diameter pile where Fig. 14 compares the load-top movement diagrams and Fig. 15 presents the shear stress-depth diagrams. The pile was allowed to float during sand placement. It will be

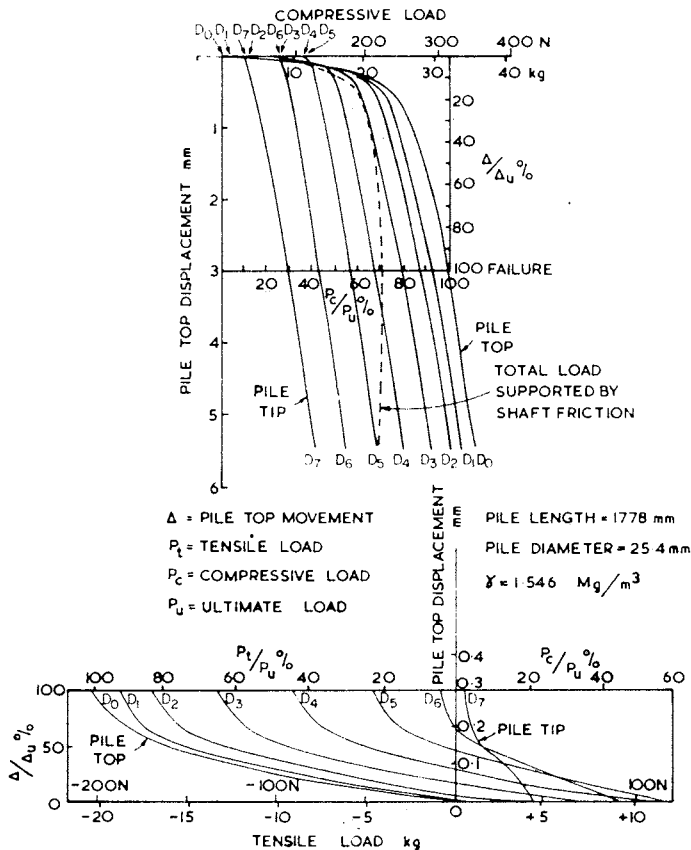


Fig. 14. Comparison of compressive and tensile load tests on a 25.4 mm diameter "floating" pile.

LONG PILES UNDER TENSILE LOADS

arching observed by VESIC (1969) around piles in compression also occurs along the lower lengths of long piles in tension. This is a significant finding in relation to the design of long piles in tension, the importance of which has been stressed by TAVENAS (1971) for bearing piles.

Figure 16 compares the average measured shear stress-depth relationships for the 25.4 mm pile in both pushing and pulling. The calculated average vertical stress in the ground has been computed using δ , the angle of pile wall friction of 25° , and an earth pressure coefficient on the pile shaft, $K_s = 0.24$. For the pile in compression the effective overburden pressure was approximately equal to the theoretical overburden pressure down to a depth of about pile mid-height. If the overburden pressure is assumed to follow a hydrostatic relation and $\tan \delta$ is constant with depth, the coefficient of earth pressure on the pile shaft, K_s , may be calculated as suggested by VESIC (1969). Values of 25° , 30° and 34° were used for δ and Fig. 17 shows the computed initial coefficient of earth pressure and that corresponding to the failure load while

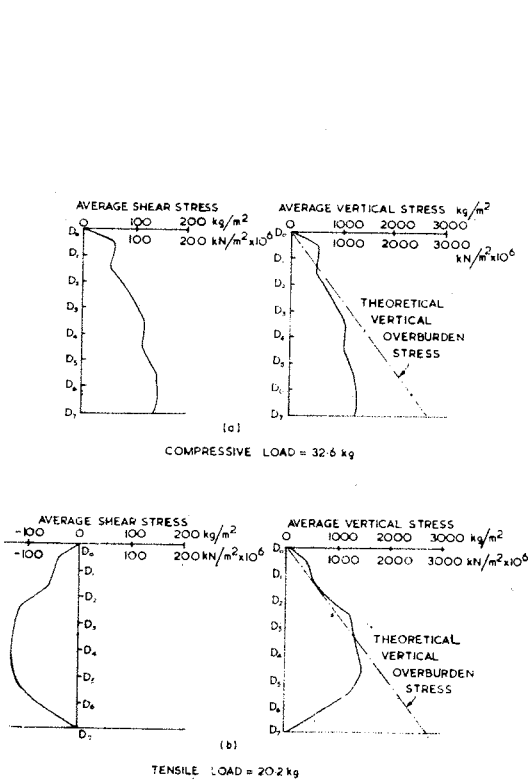


Fig. 16. Comparison of average measured shear stress/depth relationships for a 25.4 mm pile under (a) compressive loading and (b) tensile loading

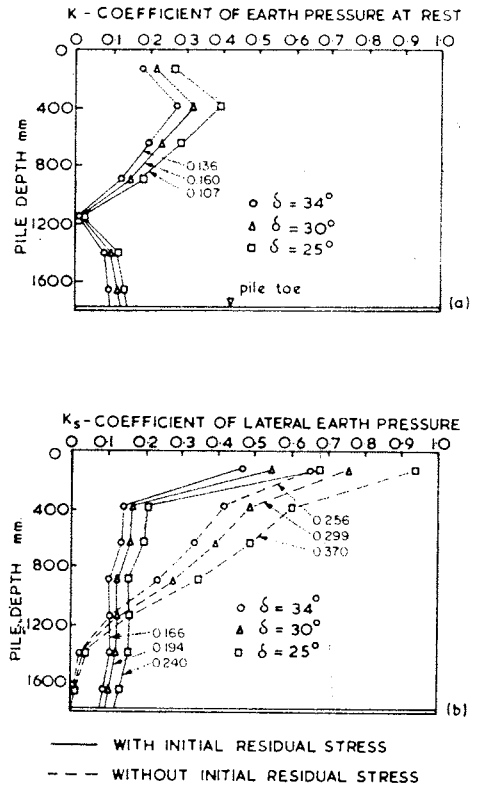


Fig. 17. Calculated earth pressure coefficients for a 25.4 mm diameter "floating" pile (a) at rest under no load, (b) at failure load— Compressive loading

Fig. 18 gives the result for the pile under a tensile load. Several points emerge: the values of K_s are very sensitive to (1) the angle of shaft friction δ , (2) the sense of load application (i.e. compressive or tensile) (3) the initial residual stress state along the length of the pile and (4) position along the length of the pile.

When piles are pushed or driven into a mass of sand it is to be expected that very different initial residual stress states will be generated along the length of the pile as well as density and stress ratio changes in the sand near to the pile. Consequently it is believed that the present test data are somewhat unreal. In the test programme this was deliberate because their primary purpose was to show the complexity of the single pile problem. This was achieved by the use of very sensitive piles, repeatable test techniques, and good control of the sand density and stress state. The simple conceptual model of pile behaviour suggested by HANNA (1969) and HANNA & TAN (1971) has been found not to disagree with the experimental observations although it requires modification in detail.

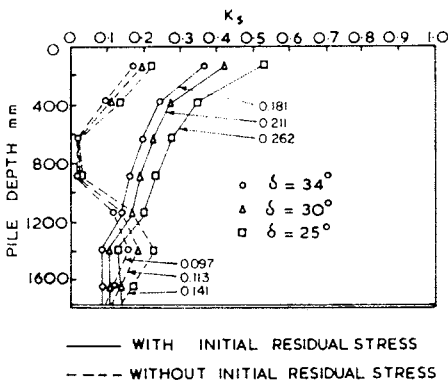


Fig. 18. Calculated earth pressure coefficients for a 25.4 mm diameter "floating" pile at failure-Tensile loading.

Because the complete understanding of the behaviour of real piles depends on many unknown factors it is essential that each potential factor be examined in detail with all of the others held constant. The present work is being extended to include (a) piles which are pushed into the sand stratum, (b) piles which are driven into the sand stratum, (c) piles subjected to a range of repeated load applications either compressive or tensile or a combination of both, (d) piles which initially are imperfect. This is a long term programme of work.

CONCLUSIONS

The tests reported in this paper show the inter-relationships between (1) arching and volume change effects which control the normal stress transmitted to the pile wall, and (2) the initial residual stress state along the pile. The results indicate the complexity of the problem and confirm that no single method of pile analysis is capable of providing an interpretation of a pile test unless it can quantify the above mentioned variables. The present study on piles in tension is a logical and supporting work of earlier studies by Vesic and other authors on piles under compressive loading.

LONG PILES UNDER TENSILE LOADS

ACKNOWLEDGEMENT

The work was carried out in the Department of Civil and Structural Engineering, University of Sheffield. The skill of the Technical Staff in the design and fabrication of the test equipment is appreciated. During the research Dr. Tan held a Goodwin Research Fellowship.

APPENDIX-NOTATION

K_s	Coefficient of Earth Pressure on Pile Shaft
L	Pile length
P	Pile load
P_b	Base load
P_c	Compressive load
P_t	Tensile load
P_u	Ultimate load
t	Pile wall thickness
δ	Angle of pile wall roughness
Δ	Pile top displacement
Δ_u	Pile top displacement at failure
γ	Sand density
ϕ_s	Pile shaft diameter
ε	Displacement of pile relative to soil
τ	Shear stress on pile/sand interface

REFERENCES

- HANNA, T.H. (1969), The Mechanics of Load Mobilization in Friction Piles, *Journal of Materials*, JMLSA, Vol. 4, pp. 924-937.
- HANNA, T.H. (1973), A Note on the Influence of Anchor Inclination on Pull-out Resistance of Clays, *Canadian Geotechnical Journal*, Vol. 10, pp.
- HANNA, T.H. and TAN, R.H.S. (1971), A Study of Load Development in Long Piles, *Journal of Materials*, JMLSA, Vol. 6, No. 3, pp. 532-554.
- HANNA, T.H. and TAN, R.H.S. (1973), The Behaviour of Long Piles under Compressive Loads in Sand, *Canadian Geotechnical Journal*, Vol. 10, pp. 311-340.
- HUNTER, A.H. and DAVISSON, M.T. (1969), Measurement of Pile Load Transfer *A.S.T.M. Special Technical Publication 444*, pp. 106-117.
- KERISEL, J. and ADAM, M. (1969), Changes Limites d'un pieu en milieux agrileux et limoneux, *Proc. 7th Int. Conf. Soil Mech. Found. Eng.*, Mexico City, Vol. 2, pp. 131-139.
- MANSUR, C.I. and Kaufman, J.L. (1958), Pile Tests, Low Still Structure, Old River Louisiana, *Trans. A.S.C.E.*, Vol. 123, pp. 715-748.
- MEYERHOF, G.G. (1963), Some Recent Research on the Bearing Capacity of Foundations, *Canadian Geotechnical Journal*, Vol. 1, pp. 16-26.
- MOHAN, D., MURTHY, V.N.S. and JAIN, G.S. (1969), Design and Construction of Multi-Underreamed Piles, *Proc. 7th Int. Conf. Soil Mech. Found. Eng.*, Mexico City, Vol. 2, pp. 183-186.

TAN AND HANNA

- NORDLUND, R.L. (1963), Bearing Capacity of Piles in Cohesionless Soils, *Proc. A.S.C.E.*, Vol. 89, pp. 1-35.
- ROBINSKY, E.I. and MORRISON, C.F. (1964), Sand Displacement and Compaction Around Model Friction Piles, *Canadian Geotechnical Journal*, Vol. 1, pp. 81-93.
- SKEMPTON, A.W. (1959), Cast-in-Situ Bored Piles in London Clay, *Geotechnique*, Vol. 9, pp. 158-173.
- TAN, R.H.S. (1971), Piles in Tension and Compression, *Ph.D. Thesis*, University of Sheffield, United Kingdom.
- TAVENAS, F.A. (1971), Load Test Results on Friction Piles in Sand, *Canadian Geotechnical Journal*, Vol. 8, pp. 7-22.
- VESIC, A.S. (1969), Load Transfer, Lateral Load and Group Action of Deep Foundations, *A.S.T.M. Special Technical Publication 444*, pp. 5-14.

AN ARRANGEMENT FOR MEASURING SWELL PRESSURES EXERTED BY EXPANSIVE SOILS

NICHOLAS K. KUMAPLEY* and GEORGE E. AFARI[†]

INTRODUCTION

Two major types of problem are generally associated with expansive soils. These are concerned with the identification of a potentially expansive soil profile and the prediction of the swell behaviour of the expansive soil under given conditions of moisture intake and loading. Extensive research into the properties of these soils in South Africa (KANTEY et al, 1952; WILLIAMS, 1958), Israel (KASSIFF et al, 1965) and America (HOLTZ, 1959; LAMBE, 1960) led to the evolution of fairly simple but reliable laboratory identification criteria for these soils. Considerable research effort has also been directed towards a study of the engineering behaviour of these swelling soils, particularly the factors which influence the magnitude and rate of development of the swell pressures generated by these soils under various conditions. In general, the magnitude of the swell pressure has been found to be a function of such factors as the type of clay mineral present, the quantity of water imbibed, the intensity of loading on the soil, the amount of expansion permitted, and the soil structure, among others.

Measurement of Swell Pressures

Current methods of measuring the swell pressure exerted by an expansive soil under given conditions make use of either the conventional laboratory oedometer or specially designed pieces of apparatus. In the method based on the use of the conventional oedometer, the soil sample is inundated and allowed to swell against a predetermined surcharge load. The soil is then loaded in the usual manner, the swell pressure being taken as the pressure necessary to recompress the soil sample to its pre-saturation voids ratio (MEANS, 1959). Alternatively, the expansion of the soil sample may be prevented by incremental loading, the swell pressure then being the maximum intensity of loading necessary to maintain the soil at constant volume. While the former technique may require a considerable length of time in the case of plastic clays, it has been found (SOM, 1968) that it is very difficult to adjust

* Lecturer in Civil Engineering, [†]Research Fellow, Department of Electrical and Electronic Engineering, University of Science and Technology, Kumasi, Ghana.

Discussion on this paper is open until 1 May, 1975.

the loading in such a way as to maintain the soil at constant volume in the latter test.

Most of the specialised arrangements proposed for the measurement of the vertical swell pressures, reviewed by KASSIFF et al, (1969), utilise either a proving ring or a proving bar in conjunction with a piston for measurement of the swell pressure while the soil sample imbibes water. The main disadvantage of this method of measuring the swell pressure is that these devices must necessarily deform by amounts generally proportional to the load being measured. This means that it is almost impossible to measure the swell pressure exerted under conditions of either null-swell or given percentage swell. This is a particularly serious disadvantage since it has been shown (SEED et al, 1962) that sample expansions of as little as 0.1% may cause a marked reduction in the measured swell pressure. LADD et al (1961) claimed to have overcome this problem by adjusting the proving ring manually to keep the sample height constant to within 0.0002 in. By far the most convenient arrangement for the measurement of swell pressures would be one which would operate automatically to keep the sample height constant at the desired value.

Automatic Swell Pressure Devices

Previous attempts at the development of automatic swell pressure devices have been reported by KASSIFF (1960) and KAZDA (1961).

These devices measure the swell pressure indirectly by determining the load required to keep the sample height constant within some narrow range as the soil imbibes water. In the Kassiff device, the load was applied through a proving ring while Kazda employed an electric motor to cause the movement of a weight along a lever to return the soil to its original thickness when it absorbed water and swelled by an amount of about 0.03 mm. The new device applies the restraining pressure hydraulically.

THE NEW DEVICE

The new arrangement uses a slightly modified hydraulic oedometer in conjunction with a Hydraulic pressure generating unit.

Hydraulic Oedometer

The hydraulic oedometer has been used for studying the consolidation characteristics of soils by LOWE et al (1964), TAN (1968) and by ROWE & BARDEN (1966) who discussed its advantages over the conventional oedometer.

TECHNICAL NOTE ON SWELL PRESSURE MEASUREMENT

The type of hydraulic oedometer used (Model WF 2450 marketed by Wykeham Farrance Engineering Ltd., England) was of the type developed at Imperial College, London, but has been modified to enable the electrical leads from the brass probes (described later) to be taken out of the apparatus. This was done by passing the leads through a short length of 1/4 in. I.D. nylon tubing which was passed through the top of the oedometer using the usual brass fittings. The space surrounding the electrical leads was filled with a plug of a sealing compound known commercially as LOCTITE. The seal provided by this compound on hardening was effective enough to prevent leakage from the oedometer. Transformer oil (TELLUS 15) was used instead of water for filling the oedometer. The reason for the choice of this type of cell fluid is discussed later.

Pressure Generating Unit

This unit is shown diagrammatically in Fig. 1. It comprises a motorised gear box which drives a threaded shaft in a screw jack to which is attached a piston moving in a water-filled cylinder. A pressure gauge has been inserted in the circuit to record the pressure generated. This unit is capable of generating and sustaining hydraulic pressures up to 1000 lb/in² (KUMAPLEY, 1969).

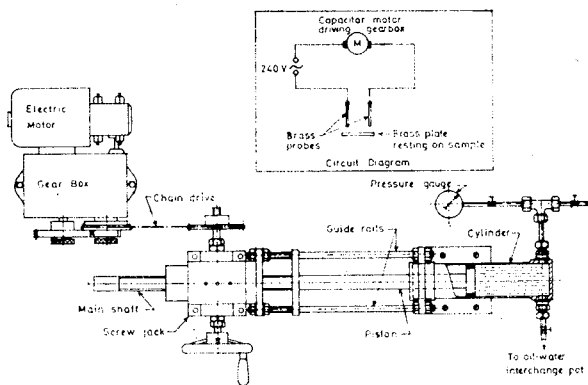


Fig. 1. A schematic diagram of the pressure generating unit.

Other Accessories

The volume of water imbibed by the soil was measured using the conventional dyed paraffin-water volume gauge (BISHOP & HENKEL, 1962) used in connection with triaxial testing. Since different liquids, namely water and transformer oil, have been used in filling the cylinder and the hydraulic

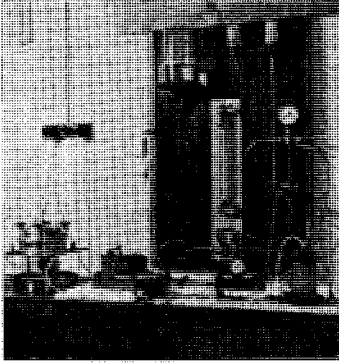


Fig. 2. General layout of the apparatus.

oedometer respectively, it was necessary to instal an oil-water interchange pot between the two units. Provision has also been made for filling the oedometer from an overhead oil container. Two self-compensating mercury constant pressure units (BISHOP & HENKEL, 1962) have been provided to enable both a back pressure and any desired surcharge to be imposed on the sample and held constant as desired. The general lay-out of the apparatus is shown in Fig. 2.

EXPERIMENTAL PROCEDURE

A stainless steel ring containing a sample of the expansive soil 0.75 in thick and 3 in. diameter, is mounted on a ceramic filter stone at the base of the oedometer. The top filter stone and the flexible (neoprene) piston incorporating the top drainage connection are installed in position (Fig. 3). A gentle suction is applied to the top drainage line to remove air trapped above the sample. A slotted brass piece $2\frac{3}{4}$ in. dia and $\frac{1}{8}$ in. thick is then placed on the neoprene piston, and a perspex bar, to which are rigidly attached two brass probes $1\frac{1}{2}$ in. long and spaced $1\frac{3}{4}$ in. apart, is mounted so that the

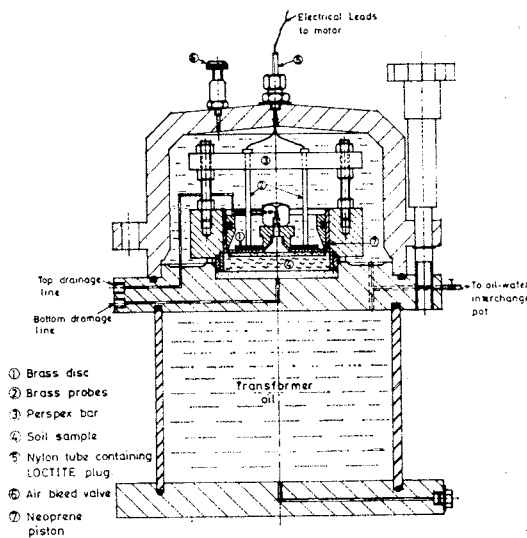


Fig. 3. A schematic diagram showing details of the hydraulic oedometer.

TECHNICAL NOTE ON SWELL PRESSURE MEASUREMENT

probes are just clear of the brass plate. For the null-swell tests, the gap between the probes and the brass plate was set at about 0.002 in. using a razor blade. The electrical leads from the electric motor, coming through the top half of the oedometer are connected to the brass probes and the top of the apparatus fitted in place, screwed down and filled with transformer oil. This type of cell fluid was chosen because of its insulating properties since it was essential to the operation of the apparatus that the electrical connection between the brass probes remains open until they make contact with the brass plate.

A seating pressure of 1 lb/in² is applied to both the cell fluid and the volume gauge, and the top and bottom drainage lines opened. At the same time, a stop clock is started and the power to the electric motor driving the hydraulic pressure generator switched on.

Mode of Operation

As the sample imbibes water and swells, the brass plate is lifted up, and as soon as it makes contact with the brass probes the electrical circuit is completed as shown by the circuit diagram in Fig. 1. The gear-box then drives the threaded shaft through the screw-jack causing the piston attached to it to move forward in the cylinder, thus generating pressure. This pressure is fed back through the oil-water interchange pot, to the oedometer to compress the soil back to its original thickness, and break the electrical contact. This process continues intermittently until the maximum swell pressure is attained. Readings of the swell pressure recorded on the pressure gauge and the volume of water imbibed are taken at various time intervals.

The main difficulty experienced with the device concerned the deterioration in the sensitivity of the contact breaking unit with time. It has been observed that after tests lasting about a week, the areas of contact of the brass probes and the brass plate were coated with a darkish compound which probably resulted from the formation of sparks during the intermittent making and breaking of the contact. The formation of this compound tended to render the electrical system of the pressure generating unit insensitive with prolonged usage, thereby causing the pressure in the oedometer to drop to low values before firm electrical contact was re-established. Work is in progress to replace this brass contact breaking unit with a mercury switch.

Other Possible Uses of the Device

By adjusting either the initial gap between the brass probes and the brass plate, or the pre-travel of the mercury switch, it is possible to investigate the

KUMAPLEY AND AFARI

effect of initial linear swell on the swell pressure subsequently developed. The controlled rate of water intake also enables the relationship between the moisture content increase and the swell pressure to be determined. Such a relationship would aid the design of structures on expansive soils in situations where the estimated final equilibrium moisture contents are much lower than saturation conditions.

Finally, using the hydraulic oedometer in its original form, it is possible to investigate the effect of various intensities of surcharge (simulating overburden pressures) on percentage swell, for various initial placement conditions.

PRELIMINARY RESULTS

Results of swell pressure measurements under null-swell conditions on undisturbed samples of a typical local expansive soil from a single borehole are given as a function of depth in Fig. 4. The sharp decrease in swell pressure with depth has also been reported by SIMPSON (1934). The rate of development of swell pressure shown in Fig. 5 is also similar to results obtained by SEED et al (1962) and illustrates the delayed nature of the development of swell pressure. Detailed results of swell pressure measurements on compacted

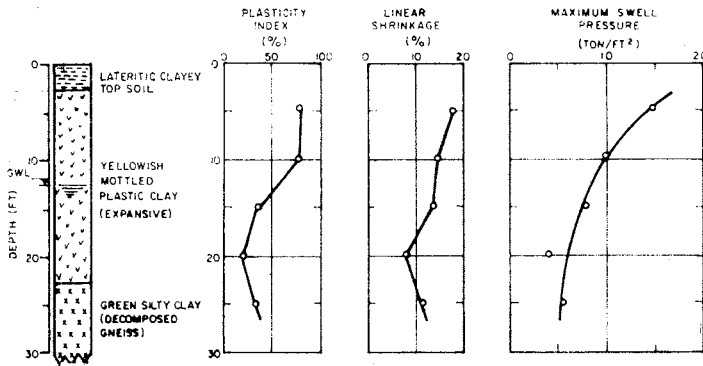


Fig. 4. Variation swell pressure with depth in yellow Cantonments Clay—East Cantonments, Accra.

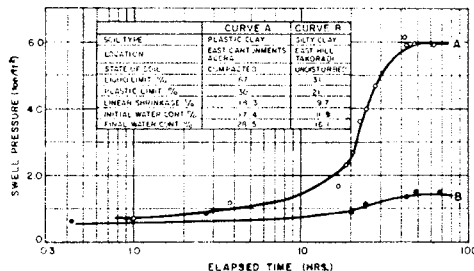


Fig. 5. The rate of development of maximum swell pressure with time.

TECHNICAL NOTE ON SWELL PRESSURE MEASUREMENT

and undisturbed samples of some local expansive soils have been reported elsewhere (KUMAPLEY & KWAMI, 1972).

CONCLUSIONS

The use of a hydraulic oedometer together with an attachment for the study of the swell behaviour of expansive soils, has been described. Preliminary results obtained have been presented and other possible uses of the device have been discussed.

ACKNOWLEDGEMENTS

The work reported out in this Note was carried out in the Civil Engineering Department of the University of Science and Technology, Kumasi. The authors wish to acknowledge the immense help received from the technicians in the workshops of the Mechanical Engineering Department in the construction of the device. Sincere thanks go to Mr. S.Y. Kwami, a final year Civil Engineering Student and Messrs. E.A. Quarcoo and I. Kavegeh, technicians in the Soil Mechanics Laboratory, for helping in the assembly of the device and the initial testing.

REFERENCES

- BISHOP, A.W. and HENKEL, D.J. (1962), *The Measurement of Soil Properties in the Triaxial Test*, 2nd Ed. Edward Arnold, London.
- HOLTZ, W.G. (1959), Expansive Clays-Properties and Problems, *Quarterly Colorado School of Mines*, Vol. 54.
- KANTEY, C.A. and BRINK, A.B.A. (1952), Laboratory Criteria for the Recognition of Expansive Soils, *Bulletin, Natl. Building Research Inst. C.S.I.R. (South Africa)* No. 9, Pretoria.
- KASSIFF, G. (1960), Swelling Pressures on Asbestos Pipes Buried in Swelling Clays, *D.Sc. Thesis, Technion, Israel Inst. of Tech.*, Haifa, Israel.
- KASSIFF, G., KORMONIK, A., WISEMAN, G., and ZEITLEN, J.G. (1965), Studies and Design Criteria for Structures on Expansive Clays, *Proc. Int. Research and Engineering Conf. on Expansive Clay Soils*, College Station, Texas.
- KASSIFF, G., LIVNEH, M. and WISEMAN, G. (1969), *Pavements on Expansive Clays*, Jerusalem Academic Press, Jerusalem, Israel.
- KAZDA, J. (1961), Study of the Swelling Pressure of Soils, *Proc. 5th Int. Conf. Soil Mech. Found. Eng.*, Paris, Vol. 1, pp. 140-142.
- KUMAPLEY, N.K. and KWAMI, S.Y. (1972), Swell Pressure Measurements on Some Expansive Accra Clays, *The Ghana Engineer*, Vol. 5.
- KUMAPLEY, N.K. (1960), Triaxial Tests on Silts and Clays at Elevated Cell Pressures, *Ph.D. Thesis, University of London*.
- LADD, C.C. and LAMBE, T.W. (1961), The Identification and Behaviour of Compacted Expansive Clays, *Proc. 5th Int. Conf. Soil Mech. Found. Eng.*, Paris, Vol. 1, pp. 201-207.
- LAMBE, T.W. (1960), *The Character and Identification of Expansive Soils*, Report to Technical Studies Programme of Federal Housing Administration, U.S.A.

KUMAPLEY AND AFARI

- LOWE, J., ZACCHEO, R.F. and FELDMAN, H.S. (1964), Consolidation Testing with Back Pressure, *Jour. Soil Mech. Found. Div., A.S.C.E.*, Vol. 90, No. SM. 4.
- MEANS, R.E. (1959), Buildings on Expansive Clay, *Quarterly Colorado School of Mines*, Vol. 54, No. 4.
- ROWE, P.W. and BARDEN, L. (1966), A New Consolidation Cell, *Geotechnique*, Vol. 16, pp. 162-170.
- SEED, H.B., MITCHELL, J.K. and CHAN, C.K. (1962), Studies of Swell and Swell Pressure Characteristics of Compacted Clay, *H.R.B. Bulletin No. 313*, pp. 12-38.
- SIMPSON, W.E. (1934), Foundation Experiences with Clay in Texas, *Civil Engineering*, Vol. 4, No. 11.
- SOM, N.N. (1968), The Effect of Stress Path on the Deformation and Consolidation of London Clay, *Ph.D. Thesis, University of London*.
- TAN, S.B. (1968), Consolidation of Soft Clays with Special Reference to Sand Drains, *Ph.D. Thesis, University of London*.
- WILLIAMS, A.A.B. (1957), Discussion on "The Prediction of Total Heave from the Double Oedometer Test" by J.E.B. Jennings and K. Knight, *Proc. Symp. Expansive Clays*, South African Inst. of Civil Engrs.

MODIFIED FAILURE CRITERIA FOR SANDS

T.S. NAGARAJ* and B.V. SOMASHEKAR⁺

INTRODUCTION

Of the three principal failure criteria for soils, the Mohr Coulomb, the Extended Tresca and Extended Von Mises, only the last two endeavour to take into account the influence of the intermediate principal stress σ_1' on strength (characterized by the angle of shearing resistance, ϕ'). Experimental results of several investigators as well as the analysis of failure criteria (BISHOP, 1966) reveal the inapplicability of these theories particularly with value of b approaching 1. With the advent of new testing techniques for testing the soils in a general stress state $\sigma_1', \sigma_2', \sigma_3'$, it is of interest to find how the influence of the intermediate principal stress can be taken into account in the theories of failure so as to give good agreement with experimental results. By an analysis of experimental data, the Extended Tresca and Extended Von Mises failure criteria have been modified in this note, the validity of which has been examined with the available published data of principal stresses at failure in a general triaxial stress system.

STRENGTH IN EXTENSION AND COMPRESSION

For comparing the values of ϕ' predicted by the three theories BISHOP (1966) formulated the following expressions:

Mohr-Coulomb $\frac{\sigma_1' - \sigma_3'}{\sigma_1' + \sigma_3'} = \text{Sin}\phi' \dots\dots\dots(1)$

Extended Tresca $\frac{\sigma_1' - \sigma_3'}{\sigma_1' + \sigma_3'} = \frac{1}{\frac{1}{3} + \frac{2}{\alpha} - \frac{2}{3}b} \dots\dots\dots(2)$

Extended Von Mises $\frac{\sigma_1' - \sigma_3'}{\sigma_1' + \sigma_3'} = \frac{1}{\frac{1}{3} + \frac{2}{\alpha} \sqrt{1 - b + b^2} - \frac{2}{3}b} \dots\dots\dots(3)$

where $\sigma_1', \sigma_2',$ and σ_3' are the major, intermediate and minor principal stresses; $b = \frac{\sigma_2' - \sigma_3'}{\sigma_1' - \sigma_3'}$ indicates the relative magnitude of σ_2' between σ_1' and σ_3' , and can take values from 0 for compression tests ($\sigma_2' = \sigma_3'$) to 1 for

* Assistant Professor, ⁺ Research Scholar, Civil Engineering Department, Indian Institute of Science, Bangalore, India.

Discussion on this technical note is open until 1 May, 1975.

extension tests ($\sigma_2' = \sigma_1'$); α is a function of ϕ' . When represented on an octahedral plane these three criteria reduce to an irregular hexagon, a regular hexagon and a circle respectively for a constant value of α .

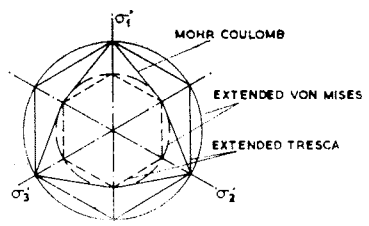
One expression for α that has been adopted by BISHOP (1966) and others is $\alpha = \frac{6 \sin \phi'}{3 - \sin \phi'}$, where ϕ' is the angle of shearing resistance in compression ($\sigma_2' = \sigma_3'$). For axial compression, $b = 0$ and, substituting these values of α and b in Eqs. 2 and 3, we find that they also reduce to $\sin \phi'$, indicating that the three theories predict the same strength in compression.

Many of the published results indicate practically identical values of ϕ' in compression and extension and for analysis in this paper this is assumed to be true. For axial extension, $b = 1$ and $\alpha = \frac{6 \sin \phi'}{3 + \sin \phi'}$ (SCHOFIELD & WROTH 1968). Substituting these values, Eqs. 2 and 3 again reduce to $\sin \phi'$ indicating same strength in axial extension also.

The equations for the extension and compression cones can be obtained from Eq. 3 and are given by:

$$\begin{aligned}
 &(\sigma_1' - \sigma_2')^2 + (\sigma_2' - \sigma_3')^2 + (\sigma_3' - \sigma_1')^2 \\
 &= 2 \left(\frac{6 \sin \phi'}{3 \pm \sin \phi'} \right)^2 \left(\frac{\sigma_1' + \sigma_2' + \sigma_3'}{3} \right)^2 \dots\dots\dots(4)
 \end{aligned}$$

These are identical to the equations given by COLEMAN (1960) by a different approach. The cones are shown in Fig. 1 on an octahedral plane. The validity



of a given failure criterion can be checked only by experimental results. Extended Tresca and Extended Von Mises criteria are examined in Table 1. It shows the percentage differences between the experimental values of the coefficient α and the coefficient computed by taking

Fig. 1. Failure surfaces on an octahedral plane. (Those shown dotted correspond to extended Von Mises and extended Tresca criteria for $\alpha = \frac{6 \sin \phi'}{3 + \sin \phi'}$).

$\alpha = \frac{6 \sin \phi'}{3 - \sin \phi'}$ for GREEN'S (1972) results. The percentage difference increases with b reaching a value as high as 53%. Thus, α cannot be taken as a constant if the criteria should be compatible with the experimental results.

MODIFIED TRESCA AND MODIFIED VON MISES FAILURE CRITERIA

As mentioned earlier, the strengths (as represented by ϕ') are assumed to be the same in extension ($b = 1$) and compression ($b = 0$). For intermediate values

TECHNICAL NOTE ON FAILURE CRITERIA FOR SANDS

of b the strength should be higher than this. The actual yield surface should thus circumscribe the Mohr-Coulomb hexagon touching it at extension and compression points.

For a general stress system we can write:

$$\alpha = \frac{q}{p} = \frac{\sigma_1' - \sigma_3'}{\frac{\sigma_1' + \sigma_2' + \sigma_3'}{3}} \dots\dots\dots(5)$$

But, $\frac{\sigma_2' - \sigma_3'}{\sigma_1' - \sigma_3'} = b$ and substitution in Eq. 5 gives:

$$\alpha = \frac{3 \left(\frac{\sigma_1'}{\sigma_3'} - 1 \right)}{\frac{\sigma_1'}{\sigma_3'} + b \left(\frac{\sigma_1'}{\sigma_3'} - 1 \right) + 2} \dots\dots\dots(6)$$

The ratio of major to minor principal stress:

$$\frac{\sigma_1'}{\sigma_3'} = \frac{1 + \sin\phi'}{1 - \sin\phi'} \dots\dots\dots(7)$$

Substitution of Eq. 7 into Eq. 6 and simplification gives:

$$\alpha = \frac{6 \sin\phi'}{2 b \sin\phi' - \sin\phi' + 3} \dots\dots\dots(8)$$

The boundary conditions, namely $\alpha = \frac{6 \sin\phi'}{3 - \sin\phi'}$ for $b=0$ and $\alpha = \frac{6 \sin\phi'}{3 + \sin\phi'}$ for $b = 1$, are satisfied for any positive power (say λ of b in Eq. 8, and therefore for generality we can write:

$$\alpha = \frac{6 \sin\phi'}{2 b^\lambda \sin\phi' - \sin\phi' + 3} \dots\dots\dots(9)$$

Thus, α should be a function of both ϕ' and b . The coefficient α for the modified theories may be written as:

$$\beta_1 = \frac{6 \sin\phi'}{3 - \sin\phi' + 2b^m \sin\phi'} \text{ (For Tresca) } \dots\dots\dots(10)$$

and $\beta_2 = \frac{6 \sin\phi'}{3 - \sin\phi' + 2b^n \sin\phi'} \text{ (For Von Mises) } \dots\dots\dots(11)$

The equations corresponding to the modified theories may be obtained by replacing α in Eqs. 2 and 3 by β_1 and β_2 respectively.

NAGARAJ AND SOMASHEKAR

Table 1. Analysis of experimental data of GREEN (1972) on Ham River sand.

Test No.	σ_1'	σ_2'	σ_3'	b	α -computed $= \frac{6 \sin\phi'}{3 - \sin\phi'}$	α -Tresca Exptl.	% Differ- ence	α -Von Mises Exptl.	% Differ- ence
Control Test	131.8	30	30	0	1.592	1.592	0	1.592	0
4	164	48.7	30	0.14	1.592	1.656	3.87	1.555	2.38
3	166.5	68	30	0.28	1.592	1.55	2.71	1.385	14.9
16	165.5	99	30	0.51	1.592	1.38	15.36	1.198	32.9
15	160	106.8	30	0.59	1.592	1.315	21.1	1.143	39.3
18	163.6	127.5	30	0.73	1.592	1.249	27.5	1.118	42.4
-	131.8	131.8	30	1.0	1.592	1.04	53.1	1.04	53.1

$$\% \text{ Difference} = \frac{\alpha\text{-experimental} - \alpha\text{-computed}}{\alpha\text{-experimental}} \times 100$$

Values of m and n in the above equations are to be determined from experimental results. Table 2 shows these being calculated for GREEN'S (1972) results. Here m and n are calculated by equating Eqs. 10 and 11 to experimentally determined coefficients, ϕ' in compression being 39° . The same table shows β_1 and β_2 calculated for average values of m and n and the percentage differences with respect to the experimental values of the coefficients. It may be noticed that the percentage differences are quite low compared to those in Table 1. Table 3 shows RAMAMURTHY'S (1973) results and the percentage differences between the experimental coefficients and the coefficients determined by the conventional method taking $\alpha = \frac{6 \sin\phi'}{3 - \sin\phi'}$. The same table shows the differences between the experimental values and the values obtained from Eqs. 10 and 11 for average values of m and n . It is at once apparent that the error is much less by the suggested method. The degree of fit to experimental data between $b = 0$ and $b = 1$ can be optimised by suitable selection of the parameters m and n .

Figure 2 shows ϕ' vs b for ϕ' in compression (= 39° for modified Tresca and modified Von Mises criteria). These are obtained by Eqs. 2 & 3 after replacing α by β_1 and β_2 respectively. ϕ' in this figure is defined according to Eq. 1.

Figure 3 shows the failure surfaces in one quadrant corresponding to the modified failure criteria. Experimental points are superimposed on the figure.

Table 2. Analysis of the results of GREEN (1972) for the calculation of m and n .

Test No.	b	α -Tresca	m	α -Von Mises	n	β_1 $m=1.92$	% Difference	β_2 $n=1.00$	% Difference
Control Test	0	1.592	2.85	1.592	-	1.592	0	1.592	0
4	0.14	1.656	2.60	1.555	1.60	1.575	4.9	1.48	4.82
3	0.28	1.55	2.37	1.385	0.99	1.525	1.61	1.385	0
16	0.51	1.38	1.83	1.198	0.73	1.39	0.73	1.25	4.34
15	0.59	1.315	1.75	1.143	0.58	1.335	1.52	1.212	6.04
-	1.00	1.04	1.00	1.04	1.00	1.04	0	1.04	0

Coefficients β_1 and β_2 are calculated using average values of m and n . α -Tresca and α -Von Mises are experimental values as in Table 1.

Table 3. Examination of experimental data of RAMAMURTHY & RAWAT (1973) based on the analysis of the results of GREEN (1972).

Exptl. No.	b	α -Tresca Exptl.	% Diff.	α -Von Mises Exptl.	% Diff.	β_1	% Diff.	β_2	% Diff.
1	0	1.61	1.12	1.61	1.12	1.592	1.12	1.592	1.12
13	0.0898	1.7	6.35	1.629	2.27	1.586	6.7	1.52	6.7
14	0.1445	1.665	4.38	1.555	2.38	1.575	5.4	1.48	4.82
15	0.186	1.66	4.1	1.53	4.05	1.56	6	1.45	5.23
16	0.2415	1.632	2.45	1.475	7.93	1.54	5.64	1.412	4.27
17	0.331	1.578	0.89	1.39	14.5	1.5	4.94	1.356	2.45
23	0.587	1.318	20.8	1.148	38.7	1.337	1.44	1.215	5.84
22	0.723	1.227	29.7	1.096	45.2	1.24	1.06	1.148	4.75
21	0.862	1.158	37.5	1.086	46.6	1.138	1.73	1.092	0.53
20	1.0	1.045	52.3	1.045	52.3	1.045	0	1.045	0

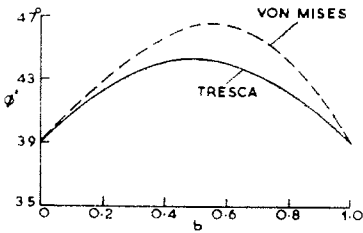


Fig. 2. Variation of ϕ' with b (ϕ' in compression = 39°) for Tresca and Von Mises criteria with modified coefficients.

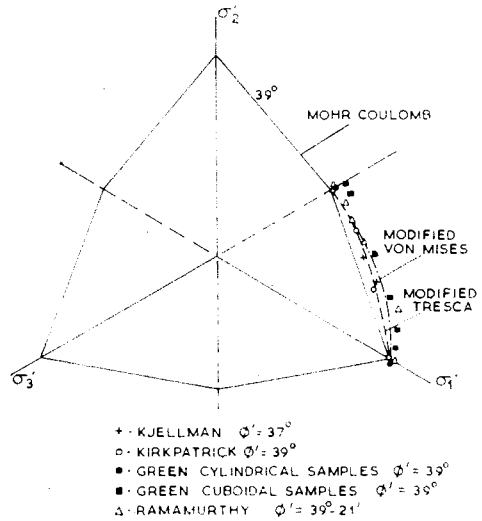


Fig. 3 Modified failure criteria on an octahedral plane.

In conclusion, α in Extended Tresca and Extended Von Mises criteria cannot be taken as a constant if they should satisfy experimental results. Modified forms of the coefficients have been suggested in this note and are shown to conform to the published experimental results.

ACKNOWLEDGEMENTS

The work reported here forms part of a study in progress on “Yield and failure of remoulded clays under general stress states”. The authors wish to express their sincere thanks to Prof. B.V. Ranganatham, Professor of Civil Engineering, for his constant encouragement. The facilities provided by the Indian Institute of Science are gratefully acknowledged.

REFERENCES

- BISHOP, A.W. (1966), Sixth Rankine Lecture, The Strength of Soils as Engineering Materials, *Geotechnique*, Vol. 14, pp. 89-130.
- COLEMAN, J.D. (1960), Suction and the Yield and Failure Surface for Soil in Principal Effective Stress Space, *Geotechnique*, Vol. 10, pp. 181-183.
- GREEN, G.E. (1972), Strength and Deformation of Sand Measured in an Independent Stress Control Cell, *Proc. Roscoe Memorial Symp.*, Cambridge, pp. 285-323.
- KIRKPATRICK, W.M. (1957), The Condition of Failure for Sands, *Proc. 4th Int. Conf. Soil Mech. Found. Eng.*, London, Vol. 1, pp. 172-178.
- KJELLMAN, W. (1936), Report on an Apparatus for Consummate Investigation of the Mechanical Properties of Soils, *Proc. 1st Int. Conf. Soil Mech. Found. Eng.*, Cambridge, Mass., Vol. 2, pp. 16-20.
- RAMAMURTHY, T. and RAWAT, P.C. (1973), Shear Strength of Sand under General Stress System, *Proc. 8th Int. Conf. Soil Mech. Found. Eng.*, Moscow, Vol. 1.2, pp. 339-342.
- SCHOFIELD, A. and WORTH, P. (1968), *Critical State Soil Mechanics*, McGraw Hill, London.

INTERNATIONAL SOCIETY NEWS

The following are some extracts of the news letters received from the Secretary General of the International Society, Professor J.K.T.L. Nash.

Professor Dusan Krsmanovic

The International Society and the Yugoslav Society for Soil Mechanics and Foundation Engineering in particular have suffered a great loss by the death of Dusan Krsmanovic in Belgrade, on 23rd March, 1974, following a long and serious illness. He was a member of the Academy of Sciences and Arts of Bosnia and Hercegovina, a professor at the Civil Engineering Faculty in Sarajevo and director of the Geotechnical Institute of that faculty.

Professor Krsmanovic was born in Sarajevo in 1908. He obtained his degree at the Civil Engineering Department of the Technical Faculty in Belgrade in 1931 where later, in 1957, he became a Doctor of Science. He was one of the founders of the Technical Faculty in Sarajevo and an outstanding teacher from the year 1950 until his death, as well as being a founder of the Geotechnical Institute. In 1961 he was elected a member of the Academy of Sciences and Arts of the Socialist Republic of Bosnia and Hercegovina. He was the author of a great number of interesting scientific works in the fields of soil and rock mechanics. His work in rock mechanics represents the basis for the development of research in this field of civil engineering. He was a member of the Yugoslav Society for Soil Mechanics and Foundation Engineering from the foundation of the Society, was its Secretary from 1954 to 1959 and held the office of President from 1959 to 1966. He was a member of the Executive Committee of the Yugoslav Society for Rock Mechanics from the foundation of that Society in 1965.

9th ISSMFE International Conference

The next International Conference is to take place in Tokyo from 11-15 July, 1977 by kind invitation of the Japanese Society for Soil Mechanics and Foundation Engineering. Preliminary planning is already well in hand and the Conference Advisory Committee is following broadly the recommendations of the MacDonald report approved at the Sydney Executive Committee in 1971. The Advisory Committee met briefly in Moscow, in 1973, extensive meetings in Stockholm in June 1974. Their initial thinking is to have four Main Sessions, four Special Lectures and twelve Specialty Sessions at the Conference which will be followed by optional tours of Japan. The detailed plans will be placed before the Executive Committee when it meets in Istanbul, 3-4 April, 1975. The Tokyo meeting of the Executive Committee is planned for 8-9 July, 1977.

SOUTHEAST ASIAN SOCIETY NEWS

The Fourth Conference on Soil Engineering

The Fourth Southeast Asian Conference on Soil Engineering will be held in Kuala Lumpur, Malaysia from 7-10 April, 1975. It is sponsored by the Southeast Asian Society of Soil Engineering, the Institution of Engineers, Malaysia and the Asian Institute of Technology. Some 50 papers by authors from various countries on a wide variety of topics have been received. Professor T.W. Lambe of Massachusetts Institute of Technology will be the guest speaker. The Society conferences present an opportunity for those interested in soil engineering to spend a few days discussing problems of mutual interest. Participants have found past conferences to be of great professional value, especially since the papers and discussions have tended to focus on problems of the region. Members wishing to attend this conference are requested to contact the Conference Secretary. All correspondence concerning the conference must be addressed to: The Hon. Secretary, IV SEACSE, P.O. Box 223, Institution of Engineers (Malaysia), Petaling Jaya, Selangor, West Malaysia.

CONFERENCE NEWS

The Fourth Southeast Asian Conference on Soil Engineering will be held in Kuala Lumpur, Malaysia from 7-10 April, 1975. It is sponsored by the Southeast Asian Society of Soil Engineering, the Institution of Engineers, Malaysia and the Asian Institute of Technology. Papers accepted include general topics of soil mechanics and engineering geology dealing with testing and site investigation, foundations, earth dams, slope stability, and roads and runways. Professor T. William Lambe will be the guest lecturer. All correspondence concerning the conference should be addressed to: The Secretary, IV SEACSE, c/o Institution of Engineers, Malaysia, P.O. Box 223, Petaling Jaya, Selangor, Malaysia.

The Sixth European Conference on Soil Mechanics and Foundation Engineering will be held in Vienna in March 1976 on the general theme Deep Foundation and Deep Excavations. The technical sessions will be:

- (1) Deep excavations; stability of temporary and permanent slopes; dewatering problems, slurry walls, walls with batter piles; bracing; freezing techniques.
- (2) Deep foundations; tunnelling.
- (3) Deep foundations in open pits; pile foundations; caisson foundations.

Titles and summaries of not more than 300 words must be submitted by 31 January 1975. All correspondence should be addressed to the Secretary, VI European Conference on S.M.F.E., A 1040 Wien, Technische Hochschule, Karlsplatz, 13, Austria.

The First Baltic Conference on Soil Mechanics and Foundation Engineering will be held at Gdansk, Poland, from 22-25 September, 1975. The theme of the conference is Geotechnics in Hydraulics and Harbour Engineering and sessions will be devoted to:

Theoretical and experimental basis of soil and rock mechanics; shallow foundations; deep foundations; stability of earth structures and structures on bed rock. The closing date for submission of papers was 30 October, 1974. Further details may be obtained from: The Secretary, 1st Baltic Conference on SM and FE, Technical University Institute of Hydro-Engineering, Maja-kowskiego Street 11, 80-952 Gdansk, P.O.B. 612, Poland.

The Fifth Asian Regional Conference on Soil Mechanics and Foundation Engineering will be held at the Indian Institute of Science, Bangalore, India from

Friday, 19 December to Monday 22 December 1975. The four Main Sessions will be on the topics: (1) Regional Deposits (2) Partially Saturated Soils (3) Foundations and Excavations (4) Structure-Soil Interaction. The closing date for the submission of the summaries of papers was 15 November, 1974. The deadline for submission of completed papers from the National Societies to the Organizing Committee is 15 March, 1975. All correspondence concerning the conference should be addressed to Dr. B.V. Ranganatham, Organizing Secretary, 5ARC, Indian Institute of Science, Bangalore, India.

Istanbul Conference on Soil Mechanics and Foundation Engineering. The Turkish National Society is organizing an international conference to take place in Istanbul from 31 March to 2 April, 1975, immediately preceding the ISSMFE Executive Committee meetings on 3rd and 4th April. The sessions will be devoted to: (1) Engineering Properties and Behaviour of Soils, (2) Case Studies of Field Behaviour, (3) Analysis and Design in Geotechnics. The conference language will be English. The closing date for submission of summaries was 30 September, 1974. The full papers must be submitted by 15 January 1975. Further particulars may be obtained from, Dr. E. Togrol, Zemin Mekanigi Arastirma Kurumu, Teknik Universite, Istanbul, Turkey.

The Sixth Regional Conference for Africa on Soil Mechanics and Foundation Engineering will be held in Elangeni Hotel, Durban from 8-12 September, 1975. The five main sessions are intended to be on: Engineering Geology and Geomorphology; Properties of Soils and Construction Materials; Foundations of Major Structures; Road and Railway Earthworks; Embankment Dams and Dam Foundations. At each of the Main Sessions there will be a General Reporter who, with a small panel, will discuss the topic and refer to papers. Formal contributions verbal discussions on printed papers will also be arranged at these sessions. The closing date for the submission of papers was 1 September 1974. Further particulars may be obtained from, The Organizing Secretary, 6th Regional Conference on Soil Mechanics, c/o, N.B. R.I., P.O. Box 395, Pretoria, 001, South Africa.

The Fifth Panamerican Conference on Soil Mechanics and Foundation Engineering will be held at Buenos Aires, Argentina from 27-31 October, 1975. The conference will consist of six main sessions on the following topics: Stress-Deformation Relationships; Special Soils: Collapsible, Expansive, Preconsolidated by Desiccation; Excavations and Deep Foundations; Tunnels in Soils; Earth and Rockfill Dams, Seismic Design of Earth and Rockfill Dams. A chairman will lead each Main Session. There will also be a General Reporter, an Adviser and a Panel of specialists. Summaries of the papers should be sent to the Organizing Committee before 31 March, 1975.

The completed papers must be submitted not later than 31 May, 1975. Further particulars may be obtained from: Senor, Secretario, Comit e Organizador; Mecanica de Su-elos e Ingenieria de Fundaciones, Ing. FERNANDO L. TORRES, C.C. 4064, Correo Central, Buenos Aires, Argentina.

The Second International Conference on Applications of Statistics and Probability to Soil and Structural Engineering will be held in Aachen, Germany from 15 to 18 September 1975. It is intended to hold four main conference sessions under the general headings of "Design Philosophy", (a) structures and (b) soils; "Design Parameters", (a) structures and (b) soils.

The closing date for the submission of summaries was 15 September, 1974. Completed papers must be submitted not later than 1 February, 1975. All correspondence concerning the conference must be addressed to: The Conference Secretariat, Deutsche Gesellschaft fur Erd-und Grundbau e.V., Kronprinzenstrasse 35 a, 43 Essen/Federal Republic of Germany.

The First International Symposium on Induced Seismicity will be held at Banff, Alberta, Canada from 15-19 September, 1975. The conference is being organized by UNESCO, the National Research Council of Canada and the Canadian Department of Energy, Mines and Resources. Full details of the programme and the procedure for submission of papers should be obtained from: ISIS Organizing Committee, c/o Institute of Earth & Planetary Physics, The University of Alberta, Edmonton, Alberta IGG 2E1, Canada.

The 25th International Geological Congress will be held in Sydney, Australia from 16-25 August, 1976. The deadline for receipt of synopsis of papers to be presented at the Congress is 30 September, 1975. The abstracts of papers must be submitted not later than 29 February, 1976. The Congress is sponsored by the Australian Academy of Sciences, The Geological Society of Australia and The International Union of Geological Sciences. Further details may be obtained from, The Secretary-General, 25th International Geological Congress, P.O. Box 1892, Canberra City, ACT 1601, Australia.

A symposium on the Engineering Behaviour of Glacial Materials will be held at the University of Birmingham from 21-23 April, 1975. The six main sessions will be on geological processes, engineering properties including fabric, glacial soils as construction materials, engineering work in glacial materials, foundation properties, and a review of investigation problems and techniques. The closing date for submission of titles and synopses of papers was August 1, 1974. Further particulars may be obtained from: The Honorary Secretary, The Midland Soil Mechanics and Foundation Engineering Society, Department of Civil Engineering, The University, Birmingham B15 2TT, England.

A Specialty Conference on In-Situ Measurement of Soil Properties will be held at North Carolina State University, Raleigh, North Carolina from 1 to 4 June, 1975. The conference is organized by the Geotechnical Engineering Division of the American Society of Civil Engineers. Session topics will include in situ measurement of: permeability; shear strength; instant stresses and deformation characteristics; volume change characteristics, including compressibility, shrink-swell potential and liquefaction potential. Deadline for submission of manuscripts is December 15, 1974. The format and length of manuscripts must conform to basic ASCE criteria, which are published in "Author's Guide to the Publications of ASCE". Model paper and a copy of the ASCE "Authors Guide" may be obtained from, Dr. Jay Langfelder, Chairman, Conference Publications Committee, 1975 ASCE GED Specialty Conference, Department of Civil Engineering, North Carolina State University, Raleigh, North Carolina 27607, U.S.A.

The Second Australia-New Zealand Conference on Geomechanics will be held in Brisbane, Australia from 21-25 July, 1975. The Conference is being jointly sponsored by: The Australian Geomechanics Society, The New Zealand Geomechanics Society, The Australian Institute of Mining and Metallurgy, The Institution of Engineers, Australia and the New Zealand Institution of Engineers.

The closing date for submission of papers was 30 November, 1974. All correspondence relating to the Conference should be addressed to: The Secretary, 2nd Australia-New Zealand Conference on Geomechanics, 157 Gloucester Street, Sydney, N.S.W. 2000, Australia.

NEWS OF PUBLICATIONS

Proceedings of the Second Southeast Asian Conference on Soil Engineering held in Singapore in June 1970, are available at a price of U.S.\$22 (inc. postage) from the Geotechnical Engineering Division, Asian Institute of Technology, P.O. Box 2754, Bangkok, Thailand. Cheques should be made payable to "Asian Institute of Technology".

Proceedings of the Fourth Asian Regional Conference on Soil Mechanics and Foundation Engineering, Bangkok, July 1971 are available in two volumes at U.S. \$35 (inc. postage) from the Geotechnical Engineering Division, Asian Institute of Technology, P.O. Box 2754, Bangkok, Thailand.

Geotechnical Abstracts: These abstracts provide a regular worldwide literature information service in the fields of soil mechanics, foundation engineering, rock mechanics and engineering geology. The abstracts are published monthly, at an annual subscription rate of DM 240, by Deutsche Gesellschaft fur Erd-und Grundbau, 35a Kronprinzenstrasse 43, Essen, Germany.

Proceedings of the Third Southeast Asian Conference on Soil Engineering, held in Hong Kong in November 1972, are now available at a price of U.S. \$25.00 (including postage by registered surface mail). Orders, together with payment should be sent to the Geotechnical Engineering Division, Asian Institute of Technology, P.O. Box 2754, Bangkok, Thailand.

Proceedings of the Specialty Session on Lateritic Soils, held at the Seventh International Conference on Soil Mechanics and Foundation Engineering in Mexico City in 1969, are available for US \$25 from the Geotechnical Engineering Division, Asian Institute of Technology, P.O. Box 2754, Bangkok, Thailand.

Proceedings of the International Conference on Land for Waste Management, held in Ottawa, Canada from 1-3 October, 1973 are now available at Canadian \$15.00 per copy and may be ordered from: Mr. M.K. Ward, Executive Secretary, International Conference on Land for Waste Management, c/o National Research Council of Canada, Ottawa, Canada KIA.

[There are six sections, one of which will be of particular interest to soils engineers, namely: Soil Properties and Processes in Relation to Waste Recycling and Disposal].

Proceedings of the Eighth Canadian Rock Mechanics Symposium held in Toronto in 1972 are now available at a price of Canadian \$5.00 per copy from: Mines Branch, Dept. of Energy, Mines and Resources, Ottawa, Canada.

Volume 1 of the Proceedings of the European Symposium on Static and Dynamic Penetration Testing, held in Stockholm, from 5-7 June, 1974 is now available at a price of Sw. Kr. 40, from: The Secretary General, ESOPT, KTH Geotechnik, S100 44 Stockholm, Sweden.

Proceedings of the Symposium on Rock Mechanics and Tunnelling Problems, held in Kurukshetra, India are now available at a price of U.S. \$25.00 from: M/S Sarita Prakashan, 175, Nanchandi Grounds, Meerut, U.P., India.

Proceedings of the Symposium on Behaviour of Earth and Earth Structures Subjected to Earthquakes and other Dynamic Loads, held in Roorkee, India in March 1973 are now available at a price of U.S. \$25.00 from: M/S Sarita Prakashan, 175—Nanchandi Grounds, Meerut, U.P., India.

Proceedings of the Symposium on Shallow Foundations, held in Bombay, India, in December 1970 are now available at a price of U.S. \$20.00 from: M/S Sarita Prakashan, 1975—Nanchandi Grounds, Meerut, U.P., India.

ASIAN INFORMATION CENTER FOR GEOTECHNICAL ENGINEERING — AGE

The **Asian Information Center for Geotechnical Engineering** (abbreviated to **AGE**) has been established within the library of the Asian Institute of Technology under the joint sponsorship of its Division of Geotechnical Engineering and the Library.

The newly established **AGE** is an invaluable source of information for all those concerned with investigation, feasibility, design and construction for all types of civil engineering projects. In addition, it is indispensable to those concerned with teaching and research in any aspect of geotechnical engineering. It is aiming to serve as a clearing house in the Asian region for information on **SOIL MECHANICS, FOUNDATION ENGINEERING, ROCK MECHANICS, ENGINEERING GEOLOGY, EARTHQUAKE ENGINEERING**, and other related fields. In cooperation with national societies, universities, governmental agencies, research organizations, engineering and consulting firms, contractors, etc., both within and outside the region, **AGE** is collecting information on all phases of geotechnical engineering research and projects, including published and unpublished reports which are of relevance to Asian conditions. **AGE** is undertaking the responsibility of designing a computer based information storage and retrieval system for the effective handling of such information, and is providing both *Current Awareness Service and Selective Dissemination of Information Service* through its publication of journal abstracts and subject bibliographies. Dissemination of collected information takes place through photocopying and micro-filming.

To ensure the effective functioning of **AGE** as an information center for geotechnical engineering in Asia, it is necessary that all organizations and individuals who are engaged in any kind of geotechnical engineering work in Asia consider **AGE** as a central depository for their information and publications regardless of language. These publications and other information will be abstracted and analyzed, and will be publicized and disseminated through **AGE**'s various channels to the benefit of the region. Among the major data files which have been stated at **AGE** are:

- (1) Data on all design, construction and research projects in geotechnical engineering of concern to the region.
- (2) Data on organizations engaged in any kind of geotechnical engineering work in the region.
- (3) Data on individuals who are engaged in any kind of geotechnical engineering work in the region.

- (4) Data on published papers and technical literature on geotechnical work of concern to the region.

Great benefit can be gained by companies and research organizations treating AGE as a central depository and service agent to provide information when it is needed.

AGE publishes the following:

- (1) *Asian Geotechnical Engineering Abstracts*: a quarterly publication consisting of abstracts of available publications on geotechnical engineering relevant to Asia.
- (2) *Asian Geotechnical Engineering in Progress*: a semi-annual publication consisting of information on current design, construction and research projects in geotechnical engineering being undertaken in Asia.
- (3) *Asian Geotechnical Engineering Directory*: a bi-annual publication consisting of information on various organizations and individuals who are doing geotechnical engineering work in Asia or relevant to Asia.
- (4) *AGE Current Awareness Service*: published quarterly to inform readers of recent geotechnical engineering publications and contents of geotechnical engineering journals received at AGE.
- (5) *AGE Journal Holdings List*: published annually to facilitate the request of photocopies.
- (6) *AGE Bibliography Series*: either recurrent or demand bibliographies published as a result of general interest or demand.

In addition to its publications, AGE provides the following three services:

- (1) *Reference Service*: for bibliographical questions.
- (2) *Referral Service*: for technical questions.
- (3) *Reproduction Service*: for photocopying or microfilming of required documents.

AGE is a non-profit making service organization. For the initial three years, it is being financially supported by a generous grant from the International Development Research Centre of Canada and by the Asian Institute of Technology. It will be necessary, however, for AGE to recover a very small portion of its operation costs from fees received on certain services. *Much can be gained through membership which is available to Individuals and Institutions at nominal fees.*

Anyone who wishes to have details about the Asian Information Center for Geotechnical Engineering should write to Dr. H.W. Lee, Director AGE, P.O. Box 2754, Bangkok, Thailand.

NOTES ON CONTRIBUTIONS TO THIS JOURNAL

Contributions to **Geotechnical Engineering** are invited from anyone. Items submitted to the Editor will be published under one of the following headings.

Original Papers

Original papers should be submitted in accordance with the *Notes for the Guidance of Authors* given inside the back cover of this journal. The Editor undertakes to acknowledge all manuscripts immediately they are received and to arrange for early review of each paper by *two* reviewers. The earliest possible publication date of contributions will be aimed for. Each author will receive 25 free copies of his paper.

Technical Notes

Technical notes will be accepted for publication. These contributions should be presentations of technical information which might be useful to the practicing or research engineer but which are not sufficient in themselves to warrant a full paper. The format to be followed for technical notes is the same as that for papers but only *two* copies need be submitted and no *Synopsis* is required. The author will receive 25 free copies of his technical note.

Reprints

Consideration will be given to reprinting papers which have been published previously but which are unlikely to have come to the attention of Society members. Only papers of a high standard which would be of particular interest to S.E.A.S.S.E. members will be considered.

Discussions

Discussion is invited on any of the papers published in this journal. The closing date for discussion is indicated at the foot of the first page of each paper. Discussions sent to the Editor may be in any form, but figures and references should comply with the general requirements for publications in this journal. *Two* copies are required.

News Items

As the official organ of the Southeast Asian Society of Soil Engineering, this journal will publish any news item of interest to the Society members. Items to be included in the next issue (June, 1975) should be sent so as to reach the Editor not later than 1 June, 1975.